HIGH BURNUP SPENT FUEL DATA PROJECT

SISTER ROD TEST PLAN OVERVIEW

Fuel Cycle Research & Development

Prepared for
U.S. Department of Energy
Used Fuel Disposition Campaign

Brady D. Hanson (PNNL)
Steven C. Marschman (INL)
Michael C. Billone (ANL)
John Scaglione (ORNL)
Ken B. Sorenson (SNL)
Sylvia J. Saltzstein (SNL)

April 29, 2016

FCRD-UFD-2016-000063
PNNL-25374

EXECUTIVE SUMMARY

This report fulfills the M2 milestone M2FT-16PN080201041, "Sister Pin Test Plan," under Work Package Number FT-16PN08020104. This report addresses comments received during the review of M3 milestone M3FT-16PN080201043, "Develop Sister Pin Test Plan."

The U.S. Department of Energy Office of Nuclear Energy, Office of Fuel Cycle Technology under the Used Fuel Disposition Campaign (UFDC) instituted the High Burnup Spent Fuel Data Project. This project obtains data to support the enhancement of the technical bases for the extended storage and transportation of high burnup (HBU) (>45 GWd/MTU) spent nuclear fuel (SNF). Under this project, a U.S. Nuclear Regulatory Commission-licensed storage cask will be loaded with 32 HBU SNF assemblies. The cask, referred to as the Research Project Cask, will be modified to allow radial and axial temperature profiles to be measured using thermocouple lances inserted through the lid. After a period of at least 10 years, the cask will be transported to a facility to be opened so the SNF can be examined and tested to provide confirmation of laboratory data that will be collected under this test plan.

In parallel with the 10-year storage of HBU SNF in the Research Project Cask, 25 HBU fuel rods have been removed either from assemblies going into the Research Project Cask or from assemblies with similar irradiation histories. These 25 "sister rods," will also be characterized and tested to:

- Determine the characteristics, material properties, and fuel rod performance of the as-received rods to provide a baseline corresponding to the condition of the SNF being loaded into a dry storage cask (i.e., post-irradiation and pool storage, but before dry storage). This is referred to as the t0 (time zero) condition and will be used for direct comparison against data to be obtained from fuel rods in the Research Project Cask when it is opened after approximately 10 years of storage, or the t10 (time 10 year) condition.
- Determine the characteristics, material properties, and fuel rod performance of the rods after they have undergone drying, helium backfill, and placement on the storage pad. This is referred to as the t0' (time zero prime) condition. These data provide an understanding of the physical changes that occur during cask loading, vacuum drying, and initial cooldown. The sister rods will be tested against the conditions as measured in the Research Project Cask as well as against conditions modeled for other dry cask storage systems that have different thermal profiles and histories. Similarly segments of sister rods will be tested under a range of hoop stresses and temperatures to account for other fuel and cask designs. The t0' data will produce information over the next 10 years to contribute to the ongoing confirmation and enhancement of the technical bases for extended storage and transportation of HBU SNF. The bulk of the testing will be done to determine the t0' data under a variety of conditions to support the surge in renewals of storage licenses expected over the next five years.

The assembly-average burnups for the 32 assemblies to be included in the Research Project Cask range from 50 to 55.5 GWd/MTU. The burnup of these assemblies is well above the average assembly-average burnup of assemblies discharged over the past decade and within 2 GWd/MTU of the most recent highest burnup assemblies discharged. Thus, other than for lead test assemblies, the burnups in this High Burnup Spent Fuel Data Project are fully representative of fuel not only discharged to date, but of expected future discharges as well.

The sister rods will be characterized and tested to examine the effects of high burnup such as increased fission gas release from fuel and decreased rod internal void volume within fuel rods, which result in an increase of the end-of-life rod internal pressure, as well as the increased oxide layer thickness of the cladding and accompanying increase in hydrogen content. None of these changes to the fuel and cladding are significant just because the burnup increased from 44 GWd/MTU (i.e., low burnup) to 45 GWd/MTU (i.e., high burnup). Rather, the changes are a continuum until significantly higher burnups are reached, though some degradation mechanisms are susceptible to occur at increasing rates when burnup increases.

The High Burnup Spent Fuel Data Project and the testing of sister rods are focused on the technical data gaps (Hanson et al. 2012a) associated with the cladding. These gaps include:

- Temperature profiles
- Stress profiles
- Drying issues
- Fuel transfer options
- Subcriticality – burnup credit
- Fuel fragmentation
- Cladding – annealing of radiation damage
- Cladding creep
- Cladding H_2 effects: delayed hydride cracking
- Cladding H_2 effects: embrittlement and reorientation.

To define the appropriate range of test parameters, UFDC performed a review of the peak cladding temperatures (PCT) and hoop stresses for standard pressurized water reactor rods. By removing the many conservatisms for calculating individual assembly decay heats and dry cask storage system temperatures, researchers found that the PCT for most HBU SNF is well below the 400°C regulatory guidance limit. The current estimate using the methodology where known conservatisms are removed for the hottest cladding temperature of any system loaded to date is only 325°C, significantly lower than that obtained using the conservative methods for licensing. At this and lower temperatures, dissolution of hydrides, a required precursor to reprecipitation and re-orientation, is limited (<100 ppm). In addition, lower temperatures reduce end-of-life rod internal pressure values, which reduce the driving force for re-orientation. Overall, these lower hoop stresses are much less likely to result in hydride reorientation, creep, or delayed hydride cracking.

Even if the cladding is brittle, a sufficient load must be applied in order to cause failure. The UFDC is performing testing and analyses to determine loads expected during extended storage and transportation. When combined with the material properties of the sister rods determined under t0, t0', and t10 conditions, testing and modeling performed under this test plan will contribute to the understanding of fuel performance under a variety of scenarios.

The laboratories performing testing on the sister rods will write test plans to provide more technical details, specifics of tests to be performed, and schedule and cost estimates.

ACKNOWLEDGMENTS

The authors thank Albert Machiels and Keith Waldrup with EPRI and Steve Nesbit with Duke Energy for their thorough review and insightful comments. The authors thank Cornelia Brim, PNNL communications specialist, for editing and formatting of the document.

CONTENTS

FIGURES

TABLES

ACRONYMS

ANL	Argonne National Laboratory
ASTM	ASTM International
BWR	boiling water reactor
CFR	Code of Federal Regulations
CIRFT	Cyclic Integrated Reversible-bending Fatigue Tester
DBTT	ductile-to-brittle transition temperature
DCSS	dry cask storage system
DHC	delayed hydride cracking
DOE	U.S. Department of Energy
DSC	dry shielded canister
EIA	U.S. Energy Information Administration
EOL RIP	end-of-life rod internal pressure
EPRI	Electric Power Research Institute
GWd	gigawatt-day
HBS	high burnup structure
HBU	high burnup
IFBA	integral fuel burnable absorber
INL	Idaho National Laboratory
INTEC	Idaho Nuclear Technology and Engineering Center
ISFSI	independent spent fuel storage installation
ISG	interim staff guidance
LWR	light water reactor
MOX	mixed oxide
MPa	megapascal
MTU	metric tons (tonnes) of uranium
NAC	NAC International, Inc.
NAIF	North Anna Improved Fuel
NRC	U.S. Nuclear Regulatory Commission
NUREG	publication prepared by staff of the U.S. Nuclear Regulatory Commission
NUREG/CR	technical report prepared by a contractor to the U.S. Nuclear Regulatory Commission
NWPA	Nuclear Waste Policy Act
NWTRB	U.S. Nuclear Waste Technical Review Board

ORNL	Oak Ridge National Laboratory
PCT	peak cladding temperature
PNNL	Pacific Northwest National Laboratory
PWR	pressurized water reactor
RCT	ring compression test
SFST	Spent Fuel Storage and Transportation (a division of the NRC)
SNF	spent nuclear fuel
SSC	structure, system, and component
TAN	Test Area North
TN	Transnuclear, Inc.
UFDC	Used Fuel Disposition Campaign
wt%	weight percent
Zircaloy	zirconium alloy
Zr	zirconium
Zry-2	Zircaloy-2
Zry-4	Zircaloy-4

REGISTRATIONS AND TRADEMARKS

M5®	Trademark of AREVA NP registered in the United States and in other countries.
ZIRLO®	Registered trademark of Westinghouse Electric Company LLC in the United States and other countries.
Optimized ZIRLO™	Trademark of Westinghouse Electric Company LLC in the United States and other countries

USED FUEL DISPOSITION CAMPAIGN
High Burnup Spent Fuel Data Project
Sister Rod Test Plan Overview

1. INTRODUCTION

In the late 1990s and early 2000s, the Dry Cask Storage Characterization Project (EPRI 2002) provided data that confirmed the performance of low burnup (<45 GWd/MTU[1]) commercial spent nuclear fuel (SNF) after ~14 years of dry storage. This project was a joint effort of the U.S. Department of Energy (DOE), the Electric Power Research Institute (EPRI), and the U.S. Nuclear Regulatory Commission (NRC). In this project, a cask that had been loaded with SNF in 1985 for thermal testing (EPRI 1986) was opened in 1999 and the fuel and internals were inspected. All of the materials, including the fuel assemblies, appeared as they did when the cask was first loaded, thus confirming the expectations based on laboratory data (EPRI 2002) that the mechanical properties of low burnup fuel undergo little change after 14 years of dry storage.

Similar data supporting the extended dry storage and transportation of high burnup (>45 GWd/MTU) (HBU) SNF are much more limited. HBU fuel assemblies, especially cladding and structural components, are subjected to higher operational duties compared to lower burnup fuel. During recent relicensing proceedings (Exelon Generation 2010; Xcel Energy 2011) for dry cask storage systems (DCSSs) and independent spent fuel storage installations (ISFSIs), the NRC raised questions on the ability of HBU SNF to maintain its integrity during extended storage and subsequent transportation. DOE and EPRI developed the High Burnup Spent Fuel Data Project to address such questions. The NRC approved (NRC 2014; NRC 2015) the license renewal applications based on an aging management program for high burnup fuel that includes evaluating the results of the High Burnup Spent Fuel Data Project, thus illustrating the need for this work.

Under the High Burnup Spent Fuel Data Project, an NRC-licensed storage cask (an AREVA TN-32B) will be loaded with 32 high burnup SNF assemblies at Dominion's North Anna Nuclear Power Station in Mineral, Virginia (EPRI 2014). The cask, referred to as the Research Project Cask, will be stored at the North Anna Nuclear Power Station ISFSI, where temperatures will be monitored and gas samples taken. After a period of at least 10 years, the cask will be transported to a facility to be opened, so that the SNF can be examined and tested to provide confirmation of laboratory data to be collected under this test plan.

In parallel with the 10-year storage of HBU SNF in the Research Project Cask, 25 HBU fuel rods (also known as "pins"), which have been removed either from assemblies going into the Research Project Cask or from assemblies with similar irradiation histories, will be characterized and tested under this test plan. These 25 rods are referred to as "sister rods" (also known as "sister pins") to indicate that they have similar characteristics as the rods against which they will be compared.

[1] GWd/MTU, gigawatt days per metric tonne uranium, is a measure of how much energy is extracted from the primary nuclear fuel source. This is typically uranium for commercial nuclear power plants.

The objectives of the sister rod characterization and testing are to:

- Determine the characteristics, material properties, and fuel rod performance of the as-received rods to provide a baseline corresponding to the condition of the SNF being loaded into a dry storage cask (i.e., post irradiation and pool storage, but before dry storage). This is referred to as the t0 (time zero) condition and will be used for direct comparison against data to be obtained from fuel rods in the Research Project Cask when it is opened after approximately 10 years of storage, or the t10 (time 10 year) condition.
- Determine the characteristics, material properties, and fuel rod performance of the rods after they have undergone drying, helium backfill, and placement on the storage pad. This is referred to as the t0' (time zero prime) condition. These data provide an understanding of the physical changes that occur during cask loading, vacuum drying, and initial cooldown. The sister rods will be tested against the conditions measured in the Research Project Cask as well as against conditions modeled for other DCSSs that have different thermal profiles and histories. Similarly segments of sister rods will be tested under a range of hoop stresses and temperatures to account for other fuel and cask designs. The t0' data will produce information over the next 10 years to contribute to the ongoing confirmation and enhancement of the technical bases for extended storage and transportation of HBU SNF. The bulk of the testing will be done to determine the t0' data under a variety of conditions to support the surge in renewals of storage licenses expected over the next five years.

This test plan overview will provide background and a higher-level overview of the work to be performed. Section 2 provides background on the low burnup demonstration; Section 3 discusses issues related to HBU SNF, including an inventory of HBU; Section 4 discusses the technical data gaps to be addressed by the High Burnup Spent Fuel Data Project and the sister rod testing; Section 5 outlines the key parameters of a test matrix; and Section 6 provides details on the 25 sister rods chosen. Specific test plans will be written by the laboratories performing testing on the sister rods to provide more technical details, specifics of tests to be performed, and schedule and cost estimates.

2. LOW BURNUP SPENT NUCLEAR FUEL DRY STORAGE DEMONSTRATION

In November 1980, the NRC issued U.S. Code of Federal Regulations Title 10, Part 72 (10 CFR 72), "Licensing Requirements for the Independent Storage of Spent Fuel and High-Level Radioactive Waste." Under this regulation, an applicant could apply for a site-specific license to place fuel in wet or dry storage in an ISFSI. In 1982, the Nuclear Waste Policy Act (NWPA) was passed by Congress and enacted January 7, 1983. Under Section 218 of the NWPA, the Secretary of Energy was directed to "…establish a demonstration program, in cooperation with the private sector, for the dry storage of spent nuclear fuel at civilian nuclear power reactor sites…" (NWPA §218(a)). This collaboration was to include "…the establishment of a research and development program for the dry storage of not more than 300 metric tons of spent nuclear fuel at facilities owned by the Federal Government…The purpose of such program shall be to collect necessary data to assist the utilities in the licensing process" (NWPA §218(c)(2)).

DOE, together with EPRI, entered into an agreement with Virginia Power (now Dominion Generation) to demonstrate a number of dry storage casks at the Idaho National Engineering Laboratory (INEL, now Idaho National Laboratory, or INL). The main purpose of this demonstration was to gain experience in loading various dry storage casks and to obtain temperature data to validate thermal models and dose measurements to ensure the shielding functioned as modeled.

The main focus of the demonstration was the CASTOR V/21 cask, the green cask shown in Figure 2-1.

Figure 2-1. Dry Storage Casks at the Idaho National Laboratory INTEC Site. Left to right: NAC-I28, CASTOR V/21, REA 2023, MC-10, VSC-17, and TN 24P. *(Photo courtesy of Idaho National Laboratory)*

2.1 Thermal Performance

The CASTOR V/21 is a cylindrical cask made of ductile cast iron that is 16 ft high and 8 ft in diameter. The external surface has 73 heat transfer fins that run circumferentially around the cask. The spent fuel basket is welded stainless steel that forms an array of 21 square channels that each holds a pressurized water reactor (PWR) fuel assembly. The lid was modified to allow insertion of thermocouple lances, each containing six thermocouples spaced axially. Seven of the 21 assemblies were instrumented with thermocouple lances and two additional lances were inserted to measure gas temperatures near the center and edge of the fuel basket.

The cask was loaded with 21 PWR assemblies from the Surry Power Station. Each assembly was a standard Westinghouse 15×15 array with 204 fueled locations, 20 guide tubes, and one central instrument thimble. The burnup of the assemblies ranged from 29.8 GWd/MTU to 35.7 GWd/MTU. Eight of the assemblies only had a cooling time of 26 months (~2.2 years) when the thermal test started in September 1985. The remaining 13 assemblies had a cooling time of 46 months (~3.8 years). The ORIGEN2 code (Croff 1980) was used to calculate the decay heat for each assembly. The eight short-cooled assemblies had decay heats of approximately 1.8 kW per assembly, whereas the longer-cooled assemblies were at or slightly above 1.0 kW per assembly. The total decay heat at the start of the thermal test was 28.4 kW. Because of the short cooling time of this fuel, the radioactive decay of short-lived radionuclides resulted in the decay heat decreasing to 27.5 kW over the one-month duration of the test. The cask was loaded using ¼-symmetry with one of the cooler 1-kW assemblies in the center.

Temperature measurements were recorded under a variety of conditions as the cask was placed in both the horizontal and vertical position and the atmosphere varied among nitrogen, helium, and vacuum. In all cases, the peak temperatures of the outer 1.8-kW assemblies were less than the center 1-kW assembly. The peak temperature measured was in the center assembly under vacuum conditions where a temperature of 414°C was measured in the guide tube. Temperatures of the center assembly and those in the middle ring were comparable, within ~20°C. However, the assemblies in the outer ring had peak temperatures ~100°C cooler.

Based on these results (EPRI 1986), the first CASTOR V/21 was loaded at the Surry Power Station in October 1986. Two key points are:

- Significant temperature gradients existed both axially and radially, so not all cladding was at the peak cladding temperature (PCT) reported.
- Newer DCSSs have improved heat transfer through the addition of materials, such as aluminum in the baskets to improve heat conduction, or through higher He pressure to increase heat convection within a canister, which results in lower internal temperatures.

2.2 Cask and Fuel Inspection

The initial licenses granted under 10 CFR 72.42(a) were limited to up to 20 years. Thus, the license at Surry was set to expire in 2006. As part of the license renewal process, the NRC sought data to support the technical basis for extended storage. This included assurance that there was no significant degradation of the fuel or DCSS that would prevent the various systems, structures, and components (SSCs) from continuing to meet their required safety functions. The CASTOR V/21 cask that was part of the initial demonstration at INL had been loaded with fuel from the Surry plant and thus was an applicable analog for the CASTOR V/21 cask at Surry.

The Dry Cask Storage Characterization Project (EPRI 2002) of NRC, EPRI, and DOE was initiated and in 1999 the CASTOR V/21 cask at INL (then the Idaho National Engineering and Environmental Laboratory, or INEEL) was opened.

The CASTOR V/21 was opened in the hot cell of the Test Area North (TAN) facility at INL. Each fuel assembly was lifted (see Figure 2-2) and the lifting force was measured to determine if assembly bowing or corrosion products caused any resistance. Very little sticking was reported. Once lifted, each assembly was then visually inspected (see Figure 2-3) to examine the relative uniformity of rod length as a sign of creep during storage; to determine the extent, if any, of fuel rod bowing; and to examine the crud and oxide layers for signs of either growth or spallation.

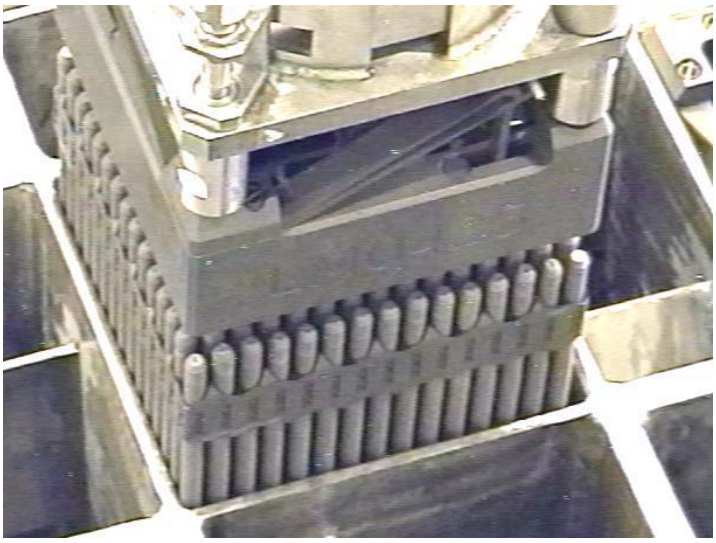

Figure 2-2. Example of Fuel Assembly Being Lifted from CASTOR V/21 (EPRI 2002)

One of the eight fuel assemblies with the highest burnup that had been located in the middle ring was chosen for further examination. Twelve individual fuel rods were extracted from the assembly, and the pull force necessary to remove each rod was measured. Each rod was then visually inspected for signs of cracks, pitting, corrosion, bowing, and for crud and oxide layer adherence. The 12 rods were then sent for additional testing.

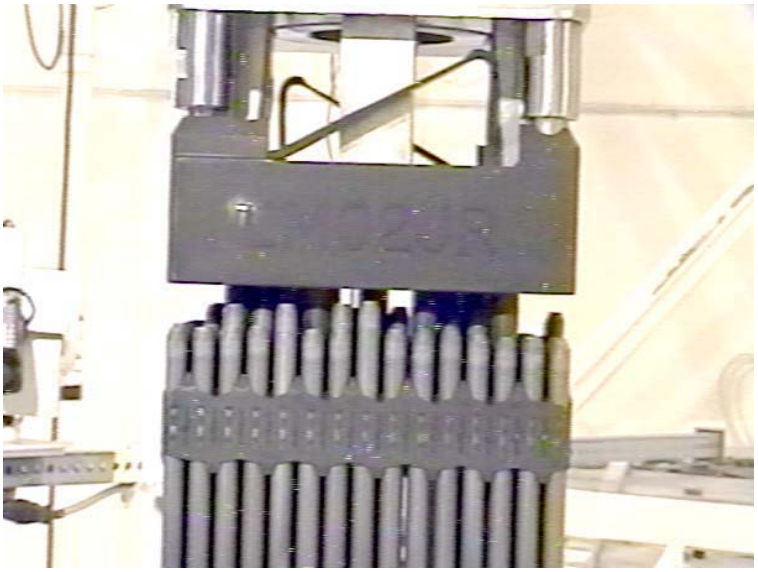

Figure 2-3. Visual Inspection of Assembly Chosen for Additional Testing (EPRI 2002)

Profilometry, where the diameter is precisely measured at four different rotational positions as a function of axial position, was performed on all 12 rods. An example of the average diameter along the length of a rod is shown in Figure 2-4. During reactor operations, the cladding "creeps down", and the diameter is thus smaller than the as-fabricated diameter. Meanwhile, the cladding oxidizes and the outside fuel rod diameter will then tend to increase as the zirconium oxide is less dense than the zirconium metal. Comparing the profilometry data before and after storage determines if creep occurred during vacuum drying or dry storage.

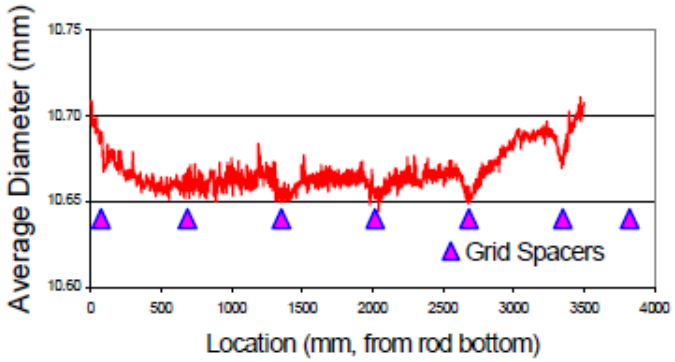

Figure 2-4 Example of Post-storage Profilometry. The nominal as-fabricated cladding diameter was 10.71 mm. (EPRI 2002)

Four of the 12 rods were then chosen to be punctured so the internal pressure, fission gas release, and void volume could be determined. The internal pressure is a key factor in calculating the hoop stress that the rod experiences. The three rods with the highest internal pressure were sectioned and sent to Argonne National Laboratory (ANL). Segments from two of the three rods were tested, first to determine the hydrogen content to look for any axial redistribution resulting

from the large axial temperature gradients during storage. Comparison of the hydrogen content at various locations before and after dry storage may be used to determine if redistribution occurs. Metallography was performed to examine oxide layer thickness, cladding thickness, hydride concentrations, and orientation. Microhardness tests were then performed to look for thermal annealing of radiation damage. If annealing occurred, the microhardness should decrease relative to that before drying and dry storage. Finally, creep tests were performed over a range of temperatures and hoop stresses to determine the residual creep life.

As documented in the final project technical report of the Dry Cask Storage Characterization Project (EPRI 2002), the conclusions were that during the 14 years in dry storage there was no evidence of significant degradation of the important-to-safety SSCs, no evidence of fuel rod failure, maximum fuel cladding creep of no more than 0.1 percent, and no evidence of hydride reorientation, and little, if any, cladding annealing had occurred. In fact, it is often stated that the cask interior and fuel appeared the same as when the cask was loaded. Based on these results, the NRC not only granted the extension for the Surry ISFSI for the additional 20 years as in the regulation, but also granted a 40-year extension (NRC 2005) under the exemption process.

3. HIGH BURNUP ISSUES

As the burnup of fuel increases, changes occur that may affect the performance of the fuel, cladding, and assembly hardware in storage and transportation. These changes include increased cladding corrosion, increased cladding hydrogen pickup, increased fission gas release, fuel-cladding bonding, and the formation of a high burnup structure (HBS) within the outer surface of the fuel pellets. Because of these changes and the limited amount of data at higher burnups, especially under in-core design basis accident conditions, the current maximum rod-averaged burnup is limited by NRC to 62 GWd/MTU. Newer cladding materials such as ZIRLO® and M5® were developed to help reduce some of these high burnup effects, notably cladding oxidation rates. However, because these materials are relatively new, available data to determine how these materials perform under storage and transportation conditions are limited.

Section 3.1 discusses the inventory of HBU SNF as discharged from U.S. nuclear power plants and Section 3.2 outlines the various issues associated with HBU.

3.1 High Burnup Inventory

It is often stated that all fuel currently being discharged or to be discharged in the near future will be HBU, having a burnup greater than 45 GWd/MTU. While the trend of increasing burnup has been true over the lifetime of commercial nuclear power, Table 3-1 shows that over the last decade, the average discharge burnup has been fairly constant. Table 3-1 shows the average assembly-average burnup for both boiling water reactors (BWRs) and PWRs discharged each year as recently reported by utilities in the GC-859 database and the U.S. Energy Information Administration (EIA 2016).

Table 3-1. Average Burnup of Assemblies Discharged by Year in the United States (EIA 2016)

	Number of Assemblies		**Average burnup (GWd/MTU)**	
Year	**BWR**	**PWR**	**BWR**	**PWR**
2000	4603	3122	38.3	44.9
2001	3617	2896	40.1	45.5
2002	4148	3765	40.2	46.0
2003	4584	3585	39.5	46.4
2004	4431	2669	42.8	46.9
2005	4075	3704	42.8	46.6
2006	3995	3516	43.1	46.9
2007	4574	2782	43.3	46.9
2008	4480	3550	43.1	47.2
2009	4395	3677	45.1	46.5
2010	4617	2856	44.3	46.8
2011	4105	3663	45.1	46.6
2012	4476	3759	45.0	44.5
2013	3246	1534	44.1	45.4
BWR = boiling water reactor, PWR = pressurized water reactor				

It is clear that, on average, many of the fuel assemblies being discharged in recent history are indeed still considered low burnup, and the projected increases in average burnup have not occurred as rapidly as predicted. One example is found in EPRI 2012 where the assumed maximum average discharge PWR burnup of 58 GWd/MTU was lowered to 55 GWd/MTU based on feedback from nuclear operating companies to the projections made just two years earlier (EPRI 2010).

An example of the number of assemblies discharged as a function of the final burnup is given in Figure 3-1. This figure covers fuel discharged through Cycle 12 at the Watts Bar Nuclear Unit 1, a large, four-loop Westinghouse-designed PWR. Cycle 1 started in February 1996 and Cycle 12 ended in March 2014. Burnups are increasing, but the maximum assembly-average discharge burnup is approximately 56 GWd/MTU. Figure 3-2 shows an example of the burnup distribution of assemblies loaded into the 32P dry shielded canisters (DSCs) [1] at the Calvert Cliffs ISFSI as of early 2013. While about 49 percent of the fuel in these 24 canisters is above 45 GWd/MTU, only one assembly exceeds 50 GWd/MTU (Calvert Cliffs 2013).

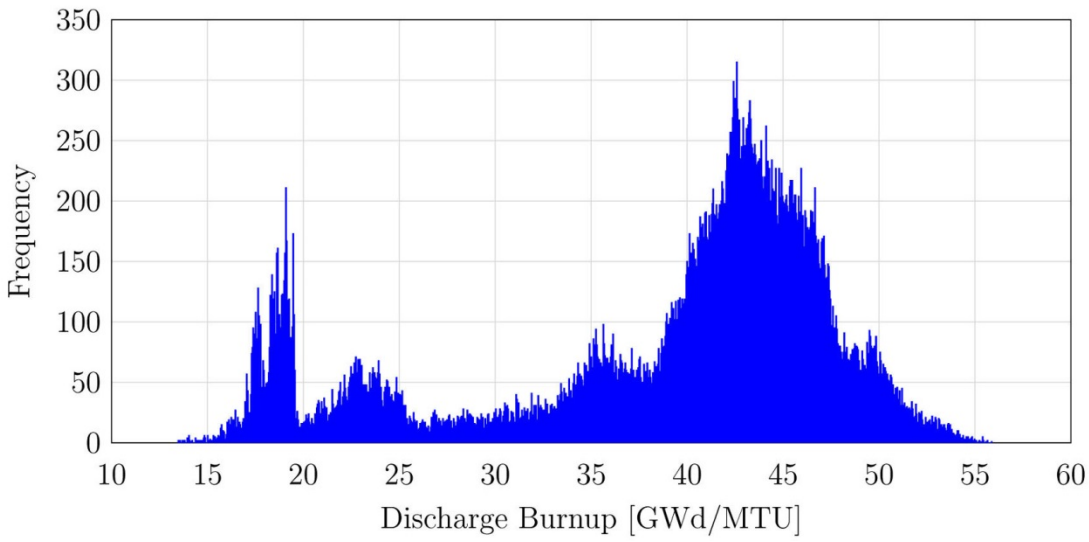

Figure 3-1. Distribution of Discharge Burnups Over 18 Years for Cycles 1-12 at Watts Bar Nuclear Unit 1 (Bratton et al. 2015)

[1] The "32P" DSC holds 32 PWR fuel assemblies. This model is produced by AREVA TN for use within their NUHOMS® Horizontal Storage Module (HSM) dry storage system.

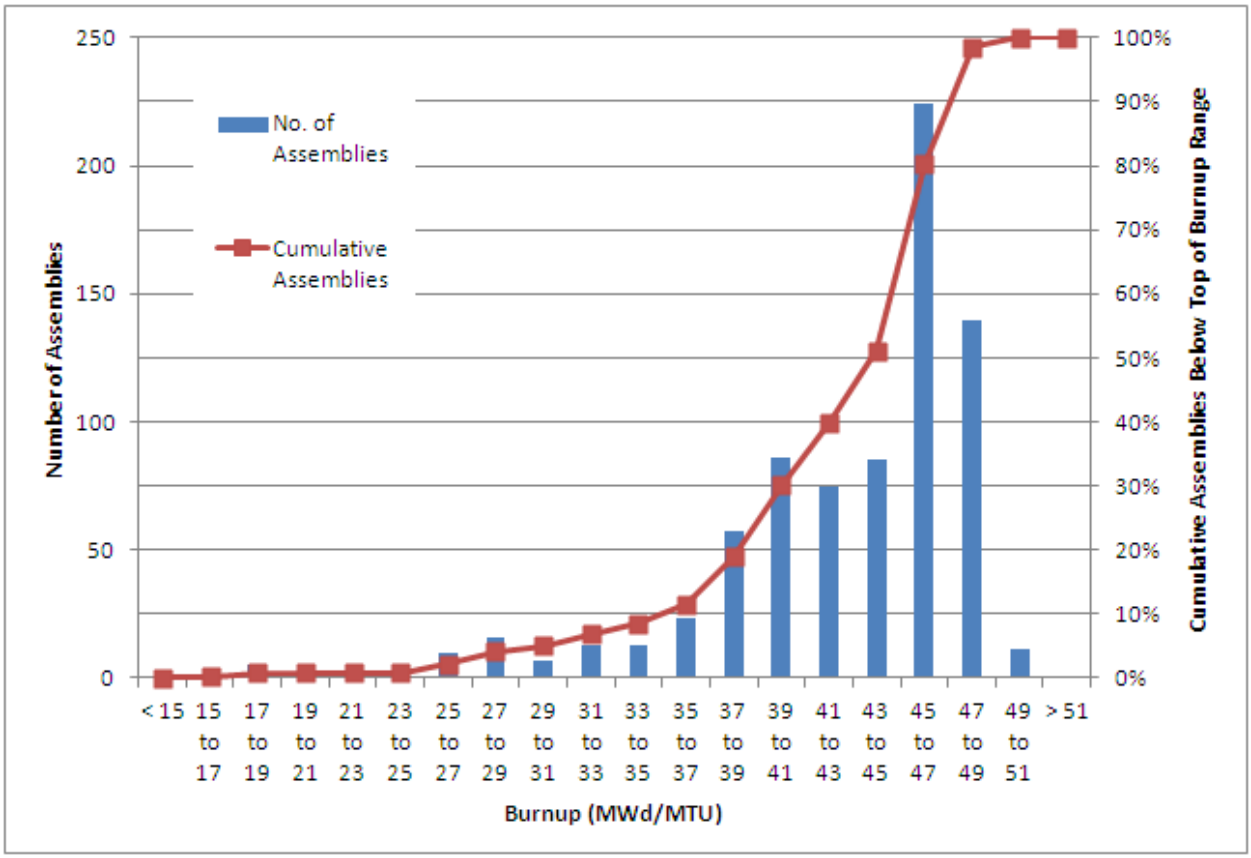

Figure 3-2. Assembly-average Burnup Distribution of Fuel Stored in the 24 Loaded 32P DSCs at the Calvert Cliffs ISFSI as of April 2013 (Calvert Cliffs 2013)

EPRI maintains a Fuel Reliability Database, and as part of the database they have been tracking discharge burnups. Table 3-2 shows the recent data and confirms that while HBU SNF is being produced, for the most part the burnup is not significantly higher than the defined 45 GWd/MTU limit.

Table 3-2. Discharged PWR Assembly Burnup 2000-2014 (EPRI 2015a)

Burnup Range (GWd/MTU)	2014 Discharges	2013 Discharges	2012 Discharges	2000-2014 Discharges
≤45	34.0%	36.5%	30.4%	38.8%
45 to ≤50	38.3%	47.5%	45.6%	43.3%
50 to ≤55	23.8%	15.5%	22.6%	16.7%
≥55	3.9%[a]	0.5%[b]	1.4%[c]	1.3%[d]

[a] Highest burnup = 56.3 GWd/MTU (20 assemblies)
[b] Highest burnup = 57.1 GWd/MTU (1 assembly)
[c] Highest burnup = 56.5 GWd/MTU (4 assemblies)
[d] Highest burnup = 70 GWd/MTU (1 lead-test assembly)

The assembly-average burnups for the 32 assemblies to be included in the Research Project Cask range from 50 GWd/MTU to 55.5 GWd/MTU (see Figure 3-3). Each cell represents an assembly identified by its unique designation , followed by the cladding alloy, the assembly-average burnup, the enrichment of ^{235}U, number of cycles the assembly was irradiated, how long it has cooled prior to emplacement in the cask, and the decay heats in watts at the time of loading and then 10 years later. The burnup of these assemblies is above the assembly-average burnups reported over the past decade in Table 3-1 and within 2 GWd/MTU of the most recent highest burnup assemblies discharged.

	1 6T0 Zirlo, 54.2 GWd 4.25%, 3cy, 11yr 1013/819W	2 (TC Lance) 3K7 M5, 53.4 GWd 4.55%, 3cy, 8yr 1167/838W	3 3T6 Zirlo, 54.3 GWd 4.25%, 3cy, 11yr 1015/821W	4 6F2 Zirlo, 51.9 GWd 4.25%, 3cy, 13yr 909/757W	DRAIN PORT
5 3F6 Zirlo, 52.1 GWd 4.25%, 3cy, 13yr 914/762W	6 (TC Lance) 30A M5, 52.0 GWd 4.55%, 3cy, 6yr 1276/832W	7 22B M5, 51.2 GWd 4.55%, 3cy, 5 yr 1637/841W	8 20B M5, 50.5 GWd 4.55%, 3cy, 5 yr 1608/827W	9 5K6 M5, 53.3 GWd 4.55%, 3cy, 8yr 1163/834W	10 5D5 Zirlo, 55.5 GWd 4.2%, 3cy, 17yr 906/797W
11 Vent Port 5D9 Zirlo, 54.6 GWd 4.2%, 3cy, 17yr 885/779W	12 28B M5, 51.0 GWd 4.55%, 3cy, 5 yr 1629/837W	13 F40 Zirc-4, 50.6 GWd 3.59%, 3cy, 30yr 696/ - W	14 (TC Lance) 57A M5, 52.2 GWd 4.55%, 3cy, 6yr 1281/835W	15 30B M5, 50.6 GWd 4.55%, 3cy, 5 yr 1614/830W	16 3K4 M5, 51.8 GWd 4.55%, 3cy, 8 yr 1162/803W
17 5K7 M5, 53.3 GWd 4.55%, 3cy, 8yr 1165/835W	18 50B M5, 50.9 GWd 4.55%, 3cy, 5 yr 1625/835W	19 (TC Lance) 3U9 Zirlo, 53.1 GWd 4.45%, 3cy, 10yr 1037/806W	20 0A4 Low-Sn Zy-4, 50 GWd 4.0%, 2cy, 22yr 725/665W	21 15B M5, 51.0 GWd 4.55%, 3cy, 5 yr 1629/837W	22 6K4 M5, 51.9 GWd 4.55%, 3cy, 8 yr 1162/803W
23 3T2 Zirlo, 55.1 GWd 4.25%, 3cy, 11yr 1036/838W	24 (TC Lance) 3U4 Zirlo, 52.9 GWd 4.45%, 3cy, 10yr 1031/802W	25 56B M5, 51.0 GWd 4.55%, 3cy, 5 yr 1628/837W	26 54B M5, 51.3 GWd 4.55%, 3cy, 5 yr 1645/846W	27 6V0 M5, 53.5 GWd 4.4%, 3cy, 8yrs 1178/844W	28 (TC Lance) 3U6 Zirlo, 53.0 GWd 4.45%, 3cy, 10yr 1035/804W
	29 4V4 M5, 51.2 GWd 4.40%, 3cy, 8yr 1109/787W	30 5K1 M5, 53.0 GWd 4.55%, 3cy, 8yr 1155/829W	31 (TC Lance) 5T9 Zirlo, 54.9 GWd 4.25%, 3cy, 11yr 1031/833W	32 4F1 Zirlo, 52.3 GWd 4.25%, 3cy, 13yr 918/765W	High Priority Assys

Figure 3-3. Final Loading Map Proposed for Research Project Cask (with assembly decay heat estimates provided by Dominion for 7/1/17 and 1/1/27)

Numerous factors affect the maximum discharge burnups fuel can achieve including, but not limited to:

- Reactor size and power
- Maximum ^{235}U enrichment limit of 5 wt% (weight %)
- Cycle length (typically 18 or 24 months in the United States)
- NRC limit of 62 GWd/MTU peak rod-average burnup
- NRC recommended limits on oxide layer thickness and hydrogen pickup
- Limits on rod internal pressure to prevent liftoff (i.e., re-opening of the fuel-cladding gap)
- Rod and assembly power to core-average power ratio
- Industry desire for zero cladding failures during reactor operation
- Economics, especially since costs increase greatly as enrichment increases.

EPRI performed an analysis of the optimum cycle length and discharge burnup as part of the DOE Nuclear Energy Plant Optimization Program (EPRI 2001). The Phase I report examined what was achievable within the 5 wt% enrichment limit. Assuming a maximum 4.95 wt% enrichment, the range of discharge burnups varies considerably, depending upon the cycle length, the period in between reactor refueling outages. For PWRs, a 24-month cycle limits the maximum achievable batch average discharge burnup to 46 GWd/MTU; for 18-month cycles the maximum batch average discharge burnup increases to almost 54 GWd/MTU. The batch average is defined as the average of the assembly-average burnups for all fuel loaded in a reactor at the same time, regardless of when they are discharged. Thus, some assemblies can be irradiated 2, 3, or 4 cycles and still be in the same batch. Higher batch average burnups can be achieved with shorter cycles because fuel assemblies are replaced more frequently and less reactivity control is needed.

Burnup for BWRs is generally lower than for PWRs largely because of natural uranium blankets on the top and bottom of the fuel stacks. Many European and Asian reactors continue to operate on a 12-month cycle where the maximum batch average discharge burnup approaches 62 GWd/MTU. The vast majority of U.S. PWRs operate on an 18-month cycle, the remainder is on a 24-month cycle; whereas almost all of U.S. BWRs operate on a 24-month cycle. Thus, it is reasonable to assume that, barring design changes addressing the factors listed above, batch average burnups in the United States could be expected to approach maximums of 54 GWd/MTU.

In reality, because of the NRC limit of 62 GWd/MTU for the peak rod-average burnup, the batch-average burnup will be limited to <52 GWd/ MTU using the methodology of Strasser et al. (1986) as reported in IZNA-3 (Adamson et al. 2004). This limit corresponds closely to the maximum batch average discharge burnup of 54 GWd/MTU for PWRs operating on an 18-month cycle.

Peak rod-average burnups are typically 5 to 9 percent higher than the assembly-average burnup (Geelhood and Beyer 2013). Where possible, a sister rod representing the peak burnup of its donor assembly was chosen for this testing program (see Section 6), so it is expected that individual rod-average burnups as high as 59 GWd/MTU will be tested. Thus, other than for lead test assemblies, the burnups in this High Burnup Spent Fuel Data Project are fully representative of fuel not only discharged to date but of expected future discharges as well.

3.2 High Burnup Effects

Higher burnup is achieved either by keeping fuel in the reactor longer, or by increasing the power density especially early in the assemblies' time in the reactor. The effect is a higher total neutron exposure and more fissions in the fuel. Similarly, the chemical reaction of the zirconium-based cladding with the cooling water increases with higher power or longer times. This section discusses the various changes in the fuel and cladding at higher burnup. None of these changes are significant just because the burnup increased to over 45 GWd/MTU. Rather, the changes are a continuum until significantly higher burnups are reached, though it is true that some degradation mechanisms are susceptible to occur at increasing rates when burnup increases. Thus, it is important to remember the relationship between the continuum of changes and the inventory and range of HBU discharges.

3.2.1 High Burnup Rim

When the cross-section averaged burnup of a fuel rod exceeds about 35 GWd/MTU, the surface microstructure of the UO_2 fuel pellet starts to change and forms what is known as the rim or HBS. Because the neutron flux (of both thermal neutrons and epithermal neutrons at the proper energy to be captured by ^{238}U) is higher at the surface of the fuel pellet, the first few hundred microns of fuel undergo more fissions than the rest of the fuel pellet. The higher burnup and cooler temperatures near the pellet surface result in the formation of the HBS. There are several characteristics in the rim zone: smaller grain size (0.1 to 0.3 μm), higher porosity (up to more than 20 percent), and larger pore size (a few microns). An example, albeit of mixed oxide (MOX) fuel, of the restructuring compared to the regular grain structure is shown in Figure 3-4.

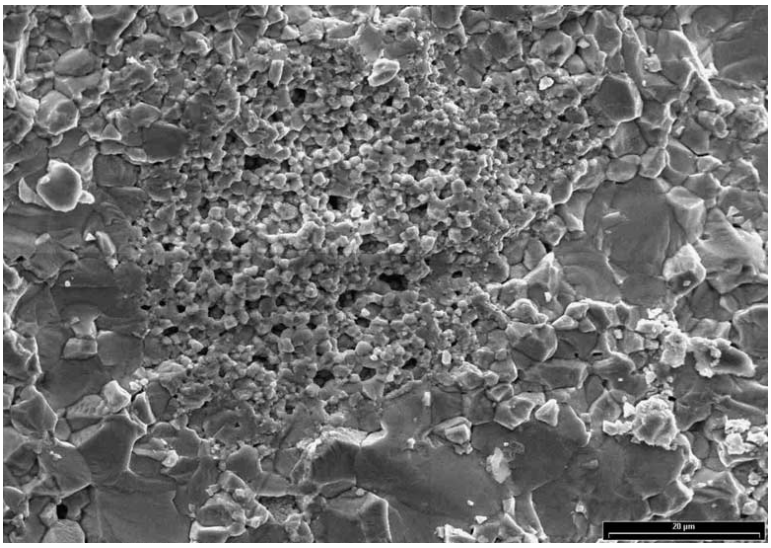

Figure 3-4. Electron Micrograph of MOX Fuel Showing Restructured Region in a PuO_2 Grain Surrounded by Grains of UO_2 With Lower Burnup and Little Porosity (Johnson et al. 2005)[1]

The thickness or width of the HBS increases with burnup as seen in Figure 3-5. A pellet with an average burnup of 50 GWd/MTU would be expected to have a rim burnup of approximately 67 GWd/MTU (Koo et al. 2001) and thus a rim thickness (from Figure 3-5) of less than 100 µm using the best estimate equation, and no more than 200 µm using the conservative equation. For a pellet with an average burnup of 60 GWd/MTU, the rim burnup would be approximately 80 GWd/MTU and corresponding rim thicknesses between 100 µm and 250 µm. Similarly, Manzel and Walker (2000) have observed HBS thicknesses of less than 200 µm for pellet burnups up to 60 GWd/MTU.

Over the range of burnups currently in the U.S. inventory, it is expected that HBU SNF will have a high burnup rim. While it has been speculated that the sub-micron grains could be released and pose a respirable dose risk upon rod breach and loss of confinement, experience has shown (Hanson et al. 2008; Wang et al. 2015) that because of pellet swelling and cladding creep down during irradiation, the fuel-cladding gap is not only closed, but the fuel and cladding are bonded together and it is very difficult to remove HBU SNF from the cladding. Some models (Raynaud and Einziger 2015) predict that the gap will open initially during dry storage because of creep; however, these models assume that temperatures of the cladding start at 400°C and they assume that all interconnected porosity within the fuel is located in the fuel-cladding gap. Submicron particles were detected when air was flowed through short fuel segments, though there was little difference between release fraction or particle-size distribution in fuels with burnups ranging

[1] Reprinted from *Journal of Nuclear Materials*,346; Johnson L, C Ferry, C Poinssot, and P Lovera; "Spent fuel radionuclide source-term model for assessing spent fuel performance in geological disposal. Part I: Assessment of the instant release fraction;" pp. 56-65; Copyright 2005, with permission from Elsevier.

from 46 to 61 GWd/MTU and air flow was much more difficult to achieve in the higher burnup segments (Hanson et al., 2008).

As part of the examination of the sister rods under this test plan, the HBS and fuel-cladding bonding will be examined, and in tests where the cladding is failed, any fuel released—including these potential sub-micron grains—will be captured and analyzed.

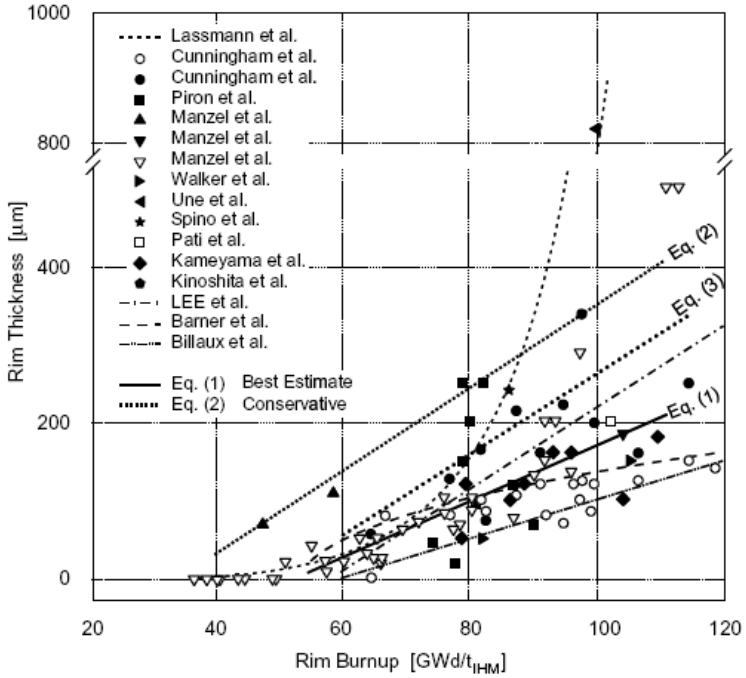

Figure 3-5. Rim Thickness as a Function of Burnup (GWd/MTU) (Johnson et al. 2005)[1]

3.2.2 Fission Gas Release

Fission gas release, mainly xenon and krypton, from the fuel pellet to the interior of the cladding is a concern if it adds to the rod internal pressure to create sufficient hoop stresses to allow hydride reorientation or cladding creep. Fission gas release is known to increase with burnup, as shown in Figure 3-6. In reality, release from the pellet is more a function of the exposure time and the rod power, and thus fuel temperature, both of which vary with time. Figure 3-6 shows results from fuel irradiated in a German PWR. Most countries in Europe operate their fuel at higher linear powers than in the United States. Thus, the magnitude of fission gas release can vary, but almost all experimental data show releases at an increasing rate starting with burnups of approximately 55 to 60 GWd/MTU. It has been shown that the increase in fission gas release at

[1] Reprinted from *Journal of Nuclear Materials*,346; Johnson L, C Ferry, C Poinssot, and P Lovera; "Spent fuel radionuclide source-term model for assessing spent fuel performance in geological disposal. Part I: Assessment of the instant release fraction;" pp. 56-65; Copyright 2005, with permission from Elsevier.

these higher burnups is not from the more porous HBS; rather the fission gas in the rim is trapped in the closed pores. Thus, the increase in fission gas release at higher burnups is not directly linked to the formation of the HBS, but it is possible that the lower thermal conductivity of the HBS results in higher pellet centerline temperatures, and thus facilitates the higher release. Finally, based on the results of the data and analyses presented by EPRI (2013), "contrary to general perception, fission gas makes a small contribution to end of life rod internal pressure," at least for the range of burnups currently licensed in the United States.

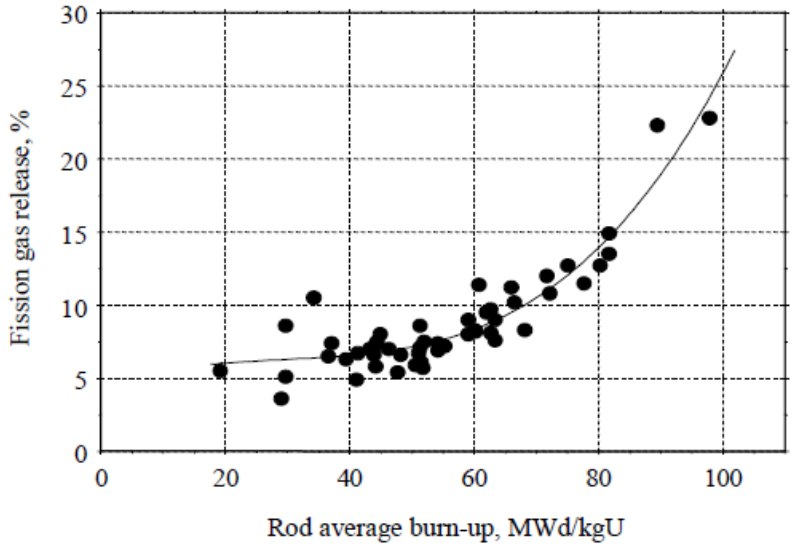

Figure 3-6. Fission Gas Release as a Function of Burnup in 15X15 PWR (Brémier et al. 2001).
(The authors are seeking permission to use this figure from the copyright owner.)

Prior to destructive examination of the sister rods, each rod will be punctured, the pressure measured, the rod free volume determined, and the gas captured and analyzed to determine the fraction and composition of any fission gas released.

3.2.3 Cladding Corrosion/Oxide Layer Thickness

During reactor operations, the Zr-based alloy cladding undergoes outer surface corrosion as the high-temperature water or steam reacts with the cladding, according to Eq. 3-1, producing a zirconium oxide layer.

$$Zr + 2H_2O \rightarrow ZrO_2 + 4H \qquad \text{(Eq. 3-1)}$$

The two major factors that affect the oxidation of PWR cladding are the water temperature and the cladding alloy type. Oxidation occurs faster at higher temperatures and thus oxide layers are thicker in higher duty (a combination of plant operating power level, temperature, and other factors) plants where the coolant temperatures are higher. This also explains why the oxide layer generally increases with increasing axial height along the fuel rods.

Figure 3-7 shows the oxide layer thickness as a function of burnup for low-tin Zircaloy 4. The plot contains more than 4,400 measurements conducted on fuel rods irradiated in reactors worldwide (EPRI 2007). The data include measurements from reactors with higher duty than is typically found in the United States and may explain some of the data above the mean. Because of the possibility of reaching the NRC limit of 100-µm oxide layer thickness within the range of burnups currently expected, industry has developed newer alloys that are more corrosion-resistant. Figures 3-8 and 3-9 show the oxide thickness as a function of burnup for these newer, niobium-containing alloys: ZIRLO®, Optimized ZIRLO™, and M5®. It is clear that these newer alloys, which account for the overwhelming majority of cladding for HBU fuel, have lower oxide layer thicknesses than the older Zircaloy-4 and low-tin Zircaloy-4 at the same burnup.

It is important to determine the oxide layer thicknesses of the sister rods at t0, as the amount of cladding thinning must be known to properly calculate hoop stresses. Samples from each of the four cladding types will be examined.

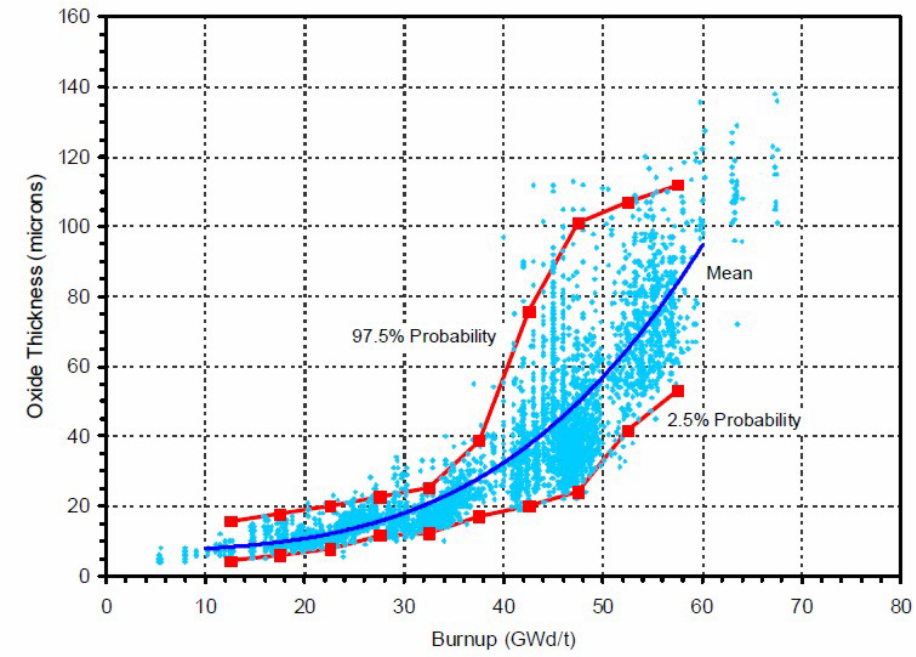

Figure 3-7. Oxide Layer as a Function of Burnup for Low-Tin Zircaloy-4 (EPRI 2007)

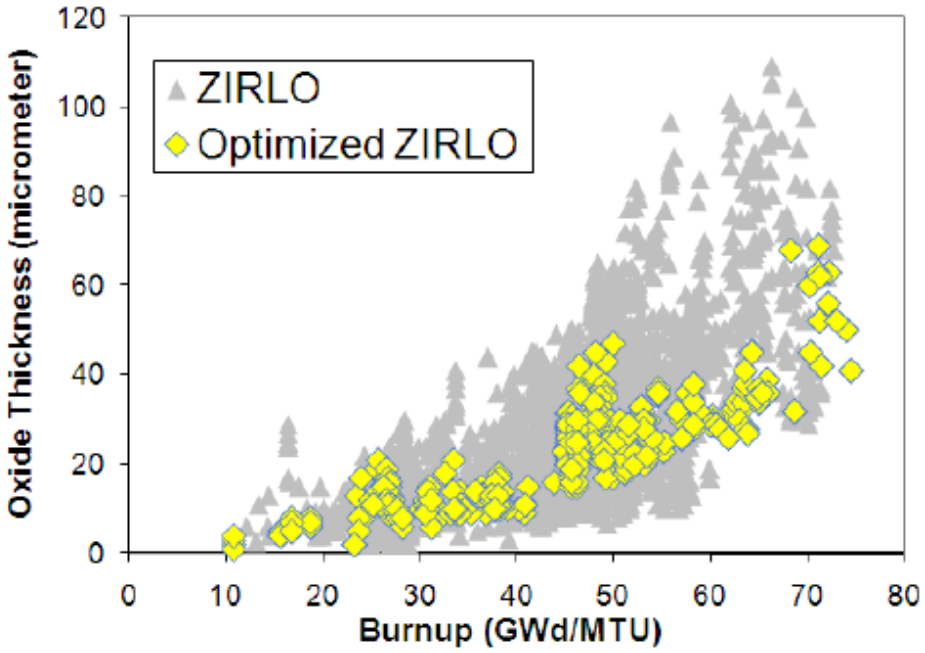

Figure 3-8. Oxide Layer as a Function of Burnup for ZIRLO® and Optimized ZIRLO™ (Pan et al. 2013) *(The authors are seeking permission to use this figure from the copyright owner.)*

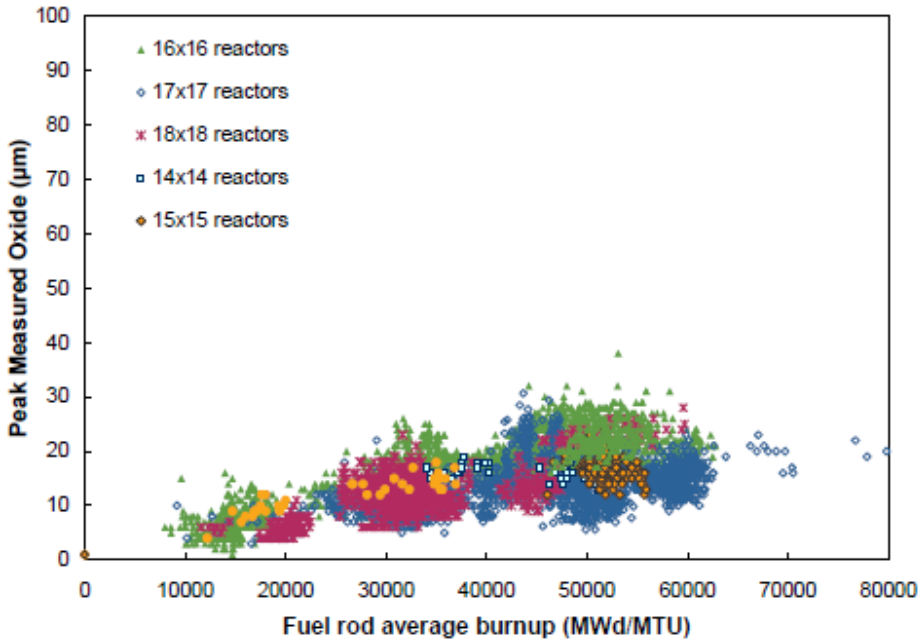

Figure 3-9. Oxide Layer as a Function of Burnup for M5® (Mardon et al. 2010)
(The authors are seeking permission to use this figure from the copyright owner.)

3.2.4 Hydrogen/Hydrides

A fraction of the hydrogen generated during the corrosion of the zirconium alloys is absorbed by the cladding. This is known as the hydrogen pick-up fraction. It follows naturally that the alloys that have larger oxide layer thicknesses will have higher hydrogen content. However, the hydrogen pick-up fraction is also different for the different alloys with the fraction somewhat higher in Zircaloy-4 than it is in either ZIRLO® or M5®. The total hydrogen content as a function of burnup for low-tin Zircaloy-4 and M5® is shown in Figures 3-10 and 3-11, respectively. There is a clear difference in the amount of hydrogen picked up by the cladding, with the newer alloys having significantly less hydrogen at the same burnup as the older Zircaloy-4 alloys.

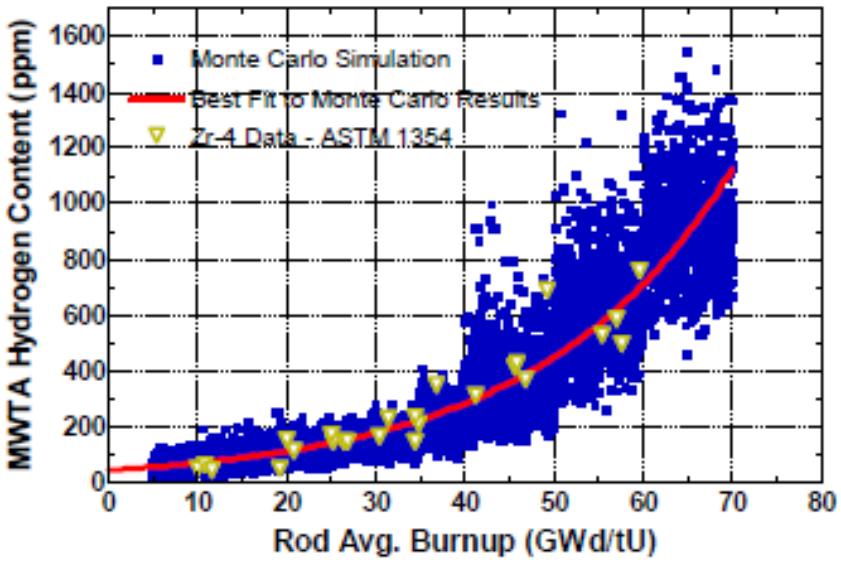

Figure 3-10. Total Hydrogen Content in Low-Tin Zircaloy-4 as a Function of Burnup (EPRI 2007)

The solubility of hydrogen in zirconium is highly temperature-dependent, with increased solubility at higher temperatures. When the concentration of hydrogen exceeds the solubility limit, zirconium hydrides form. Depending on content, size distribution, and orientation, these hydrides can embrittle the cladding by reducing ductility. Furthermore, the presence of hydrides can facilitate cracking if the hydrides are aligned radially, perpendicular to the tensile stress field. Cladding hydrides are typically observed to be oriented in the circumferential direction, but they can reorient to the radial direction, depending on the stress level in the cladding as it is cooled from a higher temperature, as will occur following the drying process or in dry storage.

Billone et al. (2013) have shown that if sufficient hydrides reorient to the radial direction with a long enough length (termed the radial-hydride-continuity factor), then the cladding exhibits a more brittle behavior below a certain temperature, referred to as the ductile-to-brittle transition

temperature (DBTT), when the cladding is subjected to a pinch-type load simulated using a ring compression test (RCT).[1] The DBTT is a function of many factors, including cladding alloy type; hoop stress; maximum temperature achieved during drying or storage; thermal history; hydrogen content; testing protocols, etc.

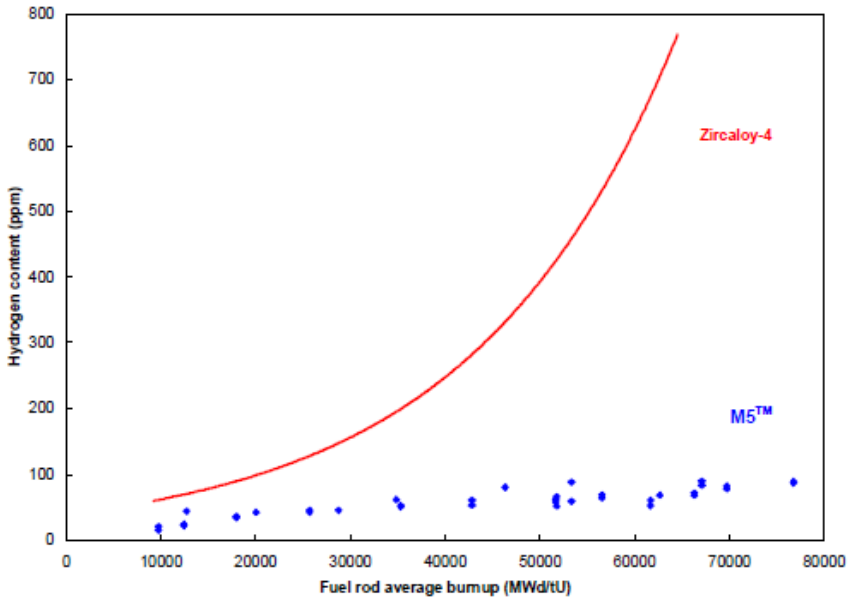

Figure 3-11. Total Hydrogen Content in M5® as a Function of Burnup (Mardon et al. 2010) *(The authors are seeking permission to use this figure from the copyright owner.)*

The primary objective of the sister rod testing is to determine the characteristics, material properties, and fuel rod behavior of the rods after they have undergone drying, helium backfill, and placement on the storage pad (referred to in this test plan overview as the t0' condition). Segments of each of the four alloy types will be subjected to a range of simulated drying conditions to span the range of PCTs expected in DCSSs, as well as a range of hoop stresses. In other instances, full-length rods will be heated to temperatures typically seen in normal dry cask storage system environments. The extent of hydride reorientation will be determined, and material properties such as the temperature- and strain rate-dependent modulus of elasticity, yield strength, ultimate tensile strength, uniform plastic elongation, and bending rigidity will be measured. The DBTT will be determined over the range of expected temperatures and hoop stresses. Together, this information will provide input to models to determine cladding performance under a variety of conditions.

[1] Clarification is needed to avoid confusing the traditional meaning of the term ductile-to-brittle transition temperature (DBTT) with the way it is being used to describe the effects of radial hydrides under pinch loading, as shown by ring-compression or ring-tensile or pressurized-tube testing. This is a direction-dependent structural behavior—not a material property—whereas the traditional usage of DBTT describes a material property regardless of how it is used in the strucure.

4. TECHNICAL DATA GAPS ADDRESSED

The Used Fuel Disposition Campaign (UFDC) under the DOE Office of Nuclear Energy, Office of Fuel Cycle Technology, performed an analysis of technical data gaps that needed to be addressed in order to contribute to the ongoing confirmation of the technical bases for extended storage and transportation of SNF, especially HBU SNF (Hanson et al. 2012a). The UFDC has been working to address these gaps, following the prioritization (Hanson et al. 2012b) first developed and then updated based on results to date (Stockman et al. 2015).

The High Burnup Spent Fuel Data Project and the testing of sister rods are focused on those gaps associated with the cladding. Because of the many different designs for DCSSs, the performance of the Research Project Cask and cask internals is secondary. This test plan only discusses gaps that will be directly or indirectly addressed through the High Burnup Spent Fuel Data Project.

4.1 Temperature Profiles

Most degradation mechanisms are temperature-dependent and, as a general rule, occur faster at higher temperatures. Industry typically employs very conservative assumptions both in calculating the decay heat of assemblies and the temperature profiles within a DCSS to ensure that PCTs are within the established regulatory guidance and technical specifications for the cask license. With these conservative assumptions, PCT predictions are significantly higher than what cladding actually experiences during drying and storage.

To address this gap, the UFDC has performed detailed thermal analyses of the Research Project Cask (Fort et al. 2016). The two different models used in the analyses have been validated previously against data obtained from other programs.

The model predictions will be compared with the data obtained from the seven thermocouple lances, each with nine axially spaced thermocouples, which will be included in the Research Project Cask (EPRI 2014). Combined with measurements of the cask external temperature and ambient conditions, these data will provide further validation of the models and show if additional model or parameter development is necessary.

4.2 Stress Profiles

The stress profiles gap is an encompassing gap meant to gather the experimental data to determine the types of stresses (magnitude, frequency, duration, etc.) imparted to various SSCs under different conditions. These conditions include normal cask handling, cask drops, seismic events (including up to design basis), cask tipover, and normal transportation. Accurate inputs and quantification of the primary stresses (from pressure and thermal loadings), secondary stresses (from residual stresses from fabrication), and external loadings (from vacuum drying, handling, and vibratory loads during transportation) are important for evaluating the material and structural response of an SSC subjected to extended storage and transportation conditions. The stress conditions, as well as further evaluation of the structural capacity and failure resistance of

the SSCs, are inexorably tied to material property inputs. Thus, it is important to obtain stresses and material properties through testing and use these data as input to models to predict cladding behavior. The importance of this gap is that even with a brittle material, a sufficient external load must be applied before the material fails.

External loads (stresses, strains, magnitude, frequency, and duration, etc.) on cladding under normal conditions of transportation are being determined via activities such as shaker table and over road tests (McConnell et al. 2015). Similarly, modeling activities (e.g., Klymyshyn et al. 2015) are examining the potential loads during extended storage.

The end-of-life rod internal pressure (EOL RIP) in the 25 sister rods, together with the extent of fuel-cladding bonding, will be determined under this test plan. Fuel performance tests, such as the Cyclic Integrated Reversible-Bending Fatigue Tester (CIRFT), will use these loads as inputs to evaluate cladding performance. Similarly, transient shock testing will be performed; shock loads determined from transportation testing will be combined with "steady state" loads to again assess performance. Data obtained from these tests will be combined with material properties determined for cladding. This information will be input to models to determine the cumulative effects of potential cladding degradation and external loads to assess cladding performance under scenarios of storage, transportation, and potentially followed by additional storage and transportation cycles.

4.3 Drying Issues

Many degradation mechanisms are dependent on or accelerated by the presence of water. Because the DCSS is loaded in a pool, it is important to remove as much water as possible during the drying process. NUREG-1536 (NRC 2010) Section 9.4.1 states "The operating procedure descriptions should facilitate reducing the amount of water vapor and oxidizing material within the confinement casks to an acceptable level to protect the SNF [spent nuclear fuel] cladding against degradation that might otherwise lead to gross ruptures." In addition to interaction with the cladding, water, water vapor, or its decomposition products produced by radiolysis can interact with the fuel, assembly hardware, baskets, neutron poisons, and canister materials. While there is no direct evidence that the amount of water that remains in a cask after a normal drying process is of concern, because of the lack of data to validate just how much water remains and the importance of water in some degradation processes, this program deems it of high importance to perform a series of tests and modeling efforts to better quantify the amount of residual water.

Gas samples will be taken from the Research Project Cask following the vacuum drying and backfill with helium during the thermal soak period in the fuel handling building (EPRI 2014). These samples will be analyzed for water vapor to provide experimental data to help determine the amount of residual water remaining following approved drying and handling procedures.

4.4 Fuel Transfer Options

This gap addresses potential technical issues and effects of rewetting and redrying, including repeated thermal cycles, fuel with particular emphasis on potential changes in hydride distribution and orientation and the effects of these changes on cladding behavior. For a cask loaded at an ISFSI, the question of the effects of rewetting of the SSCs and the effect on material properties becomes relevant if the cask has to be reopened in a pool. One concern is that pools are typically around 30°C or less and at those low temperatures additional hydrides may precipitate in the cladding and potentially alter the properties compared to what they were during storage. Another concern is that crud or oxide layers may spall, again affecting the analyses. Even if rewetting is determined to have minimal or no effect on the properties to be measured, the cask and its contents must be redried. Redrying is a potential issue if the cladding is hot enough that degradation, such as creep or hydride reorientation, can occur in addition to any degradation from the initial drying process.

While there is still interest in the effects of rewetting, multiple drying cycles, and any potential "memory" effect of hydride orientation, given the lower PCTs now estimated (see Section 5.1), it is not believed that subsequent redrying at even lower temperatures will have any effect.

Under this test plan, some tests to examine the effects of redrying and multiple thermal cycles may be performed to confirm this hypothesis.

4.5 Subcriticality – Burnup Credit

Burnup credit is allowance in the criticality safety analysis for the decrease in fuel reactivity resulting from irradiation. The level of burnup credit depends on the isotopes modeled in the criticality analysis. Actinide-only burnup credit generally refers to modeling only actinides with the highest reactivity worth. Full burnup credit refers to a combination of the uranium and plutonium isotopes evaluated in actinide-only burnup credit, plus a number of fission products and minor actinides.

The NRC staff guidance for burnup credit in the criticality analysis of PWR SNF storage and transportation is provided in SFST-ISG-8 Rev. 3 (NRC 2012), which has recently been updated based on the latest data and associated analyses and models developed domestically and internationally. This update includes guidance for full burnup credit including the significant actinides and fission products. This update also allows for reliance on a misload analysis (i.e., the placement of assemblies into a SNF storage or transportation system that do not meet the approved loading criteria) in lieu of SNF assembly burnup measurements prior to loading.

Radiochemical analyses from various axial locations of the sister rods may be performed as a way to provide additional data in order to reduce the uncertainty in the existing sets of isotopic data applicable to current PWR SNF burnup credit modeling approaches.

4.6 Fuel Fragmentation

The concern with fuel fragmentation is that under various accident scenarios, such as cask drop or tipover, the fuel might fragment or break into small, respirable-size particles and pose both a retrievability and dose issue (Einziger and Beyer 2007). This may be especially true given the small particle size of the restructured rim or HBS discussed in Section 3.2.1.

To address this gap, tests that are performed with fuel still in the cladding (e.g., CIRFT, RCT, and tube burst, etc.) will be configured to capture and analyze the amount and particle size of the fuel released upon failure of the sample.

4.7 Cladding – Annealing of Radiation Damage

Dislocations form in Zircaloy-based cladding as a result of radiation damage from fast neutron interaction. These dislocations result in a rapid increase of strength and corresponding decrease in ductility. However, these changes basically saturate after the first cycle in a reactor, so higher burnup makes little difference. Thermal annealing of the radiation damage would restore ductility and lessen the likelihood of failure when subjected to an external load. Annealing is known to occur relatively quickly at temperatures above 400°C. Ito et al. (2004) have found that in Zircaloy-2 and Zircaloy-4, nearly 50 percent hardness recovery, as measured by micro-Vickers hardness tests, occurred at 360°C over approximately 0.9 years. At 330°C, recovery occurred over the same time frame, albeit at a much slower rate. This suggests that even at the lower temperatures now being predicted for most dry storage systems, ductility will slowly be restored over the years of storage. This may explain the DBTT behavior reported by Billone et al. (2015) where at high hoop stress, the DBTT for a sample heat-treated at 350°C for a few hours was higher than the DBTT for a sample heat treated to 400°C. Bouffioux et al. (2013) have seen that annealing strongly reduced the adverse effects of radial hydrides.

Long-term annealing tests at these lower temperatures may be performed on the different cladding alloys to determine if restoration of ductility can be expected over longer times at the temperatures typical for DCSSs. Micro-hardness tests may be performed on the t0, t0', and long-term annealed cladding, such as t10 conditions, to determine if annealing under relevant conditions occurred.

4.8 Cladding Creep

Previously, creep to rupture was considered to be the most likely failure mode during dry storage (Adamson 2004). Creep occurs most likely early in the dry storage lifetime when the temperatures and cladding stresses are at their highest. However, thermal creep is considered to be self-limiting because if the cladding creeps, the volume expands, thereby reducing the RIP and stress and limiting additional creep. Given the lower PCT temperatures now estimated (see Section 5.1) as well as the correspondingly lower hoop stresses (see Section 5.2), thermal creep is expected to be minimal. Other potential sources of cladding stress are helium released during

the alpha decay of some transuranic radioisotopes over time or pellet swelling. Raynaud and Einziger (2015) examined this possibility for HBU SNF over a period of 300 years of dry storage and determined that maximum creep strains accumulated were on the order of 0.54 to 1.04 percent. Since creep failures are not expected below at least 2 percent strain, these other sources of stress are not considered important for extended dry storage. It is possible that viscous creep mechanisms over long times could be in play; however, less than 0.1 percent creep was observed in the Dry Cask Storage Characterization Project (EPRI 2002) over ~14 years when thermal creep dominated.

Long-term creep will be examined as part of the High Burnup Spent Fuel Data Project.

The t0 profilometry data obtained on the HBU sister rods will be used to compare against profilometry results on rods extracted from the Research Project Cask after approximately 10 years (t10) to determine if creep occurred during vacuum drying or dry storage. The EOL RIP as well as the rod void volumes in the 25 sister rods, together with the extent of pellet-cladding bonding, will be determined under this test plan. Some have hypothesized that the effect of such bonding could limit cladding deformation in response to gas-pressure, axial-bending, and pinch-type loading.

4.9 Cladding H_2 Effects: Delayed Hydride Cracking

Delayed hydride cracking (DHC) is a time-dependent mechanism traditionally thought of as diffusion of hydrogen to an incipient crack tip (flaw), followed by nucleation, growth, and fracture of the hydride at the crack tip. The process continues as long as a sufficient stress to promote the hydrogen diffusion occurs. DHC has traditionally been ruled out as a possible mechanism for cladding degradation during extended storage because as the temperatures decrease, the stress decreases and becomes insufficient to promote crack propagation. Raynaud and Einziger (2015) analyzed the critical flaw size required to trigger DHC and found the critical flaw size far exceeded any realistic flaw size expected in cladding at the end of reactor life. Kim (2008) proposed that cladding is more likely to fail by DHC at temperatures below 180°C, but sufficient stress risers or incipient crack size are still necessary and neither are expected to exist in typical dry storage.

Based on these analyses, no specific tests to look for DHC will be performed. Rather, if any rods fail (as will be detected by fission gas in the cask) during the storage or transport of the Project Research Cask to the facility where it will be opened, the rod(s), if they can be located, will be examined to determine the cause. Comparison of hydrogen and hydride distributions against the t0 and t0' data will determine if DHC was involved.

4.10 Cladding H_2 Effects: Embrittlement and Reorientation

During reactor operations, water corrosion of zirconium-alloy cladding produces hydrogen, some of which is taken up by the cladding. When the amount of hydrogen exceeds the solubility limit

at a given temperature, the hydrogen precipitates as zirconium hydrides. In most cladding alloys, these hydrides precipitate predominately in the circumferential direction. Because of the relatively cold (typically <35°C) temperatures of the spent fuel pools, most of the hydrogen is precipitated as hydrides, and very little, if any, additional corrosion and hydrogen uptake occurs. When the fuel is loaded into a DCSS, it undergoes a drying operation to remove water from the canister/cask. During the drying operation, the cladding temperature increases because the heat transfer under vacuum conditions is limited. As the temperature increases, some of the zirconium hydrides dissolve: the higher the temperature gets, the more hydrides dissolve. As the cladding cools over time, the hydrogen in solid solution in the cladding eventually reprecipitates back in the form of zirconium hydrides.

When the hoop stress in the cladding is sufficiently high during cooling, a fraction of the reprecipitated hydrides will be oriented in the radial direction. Radial hydrides can reduce failure stresses and strains in response to hoop-stress loading, thereby making the cladding more susceptible to damage under *pinch* loading conditions, especially in the lower temperature ranges. The transition temperature at which ductility drops below a certain level has been referred to as the DBTT[1]. If the cladding is subjected to external pinch-loading loads, either during extended storage or transportation, when the temperature is still above the DBTT, the cladding still exhibits ductile behavior. Even if the temperature is below the DBTT, the external load transferred to the cladding must still be sufficient to cause the cladding to fail. Cladding may experience this same transition from ductile-to-brittle response even without radial hydride formation when the hydrogen content is very high.

The DBTT is a function of many factors, including cladding alloy type, peak hoop stress, PCT, temperature and stress histories, hydrogen content, and testing protocols, etc. Given the expected lower realistic temperatures during drying and storage, the lower hoop stresses, and the bulk of the fuel having burnups less than 55 GWd/MTU, it has been hypothesized that embrittlement and hydride reorientation is possible, but unlikely to be degrading. A comprehensive test program using the four different cladding types of HBU SNF of the sister rods will be performed to assess when hydride embrittlement and reorientation could become an issue under the conditions expected for dry storage.

This comprehensive program includes, but is not limited to:

- Measurement of the EOL RIP and void volume in each of the 25 sister rods together with oxide layer thicknesses and profilometry, so accurate, local hoop stresses can be calculated.
- Hydride concentration and orientation for both t0 and t0’ (after cooling) conditions at various axial locations and for individual test specimens can be determined.

[1]The transition from ductile-to-brittle behavior is due primarily to the combined effects of brittle hydrides oriented nearly (within ±40°) perpendicular to the stress field and of a hardened zirconium-alloy matrix.

- RCT for both t0 and t0' conditions where the PCT and hoop stress are varied over the range representative of conditions in the Research Project Cask as well as other representative systems loaded with HBU SNF that may experience higher PCT. This will allow the range of DBTTs to be determined for each cladding type under representative conditions.
  - Some tests will be repeated using segments with the fuel still in the cladding to determine the degree to which the fuel limits cladding displacement under pinch-type loading, and thus limits cladding stresses and strains.
- CIRFT using the loads for scenarios under extended storage and normal conditions of transportation can be used to determine the performance of cladding with various hydride concentrations and orientations.
  - Transient shock testing will be performed where shock loads determined from transportation testing will be combined with "steady state" loads to again assess performance.
- Determination of material properties of cladding in both t0 and t0' conditions following ASTM-approved methodologies to examine the effect of hydrides and potential hydride reorientation on those properties. These properties are used in models to predict performance under a variety of conditions that cannot be tested. It is important to measure these properties in a relevant temperature range because they are not available for current PWR cladding alloys.
  - A combination of tube tensile, tube compression, and tube burst tests will be performed as these geometries replicate best the geometry of a fuel rod.
  - Some tests will be repeated with fuel still in the cladding to determine if the fuel/cladding bonding affects how the cladding responds to the external forces.

5. TEST MATRIX

The laboratory performing testing will develop specific test plans outlining the specific tests to performed and under what conditions. This section of the overview provides high-level guidance for key parameters in the test matrix.

5.1 Temperature

For regulatory purposes, it is often assumed that actual PCTs in dry storage are close to 400°C. One reason for this assumption is the 414°C measurement taken in the CASTOR V/21 cask test as discussed in Section 2.1. However, as noted previously, that test had very short-cooled fuel (all less than four years and eight assemblies of only 2.2 years), whereas typical loadings have fuel cooled at least five years. In addition, modern DCSS designs are very efficient at transferring heat. When the conservative assumptions used for actual (versus limiting) spent fuel inventory, decay heat calculations and thermal modeling are removed, actual PCT and system temperatures are much lower than generally assumed. Still, it is important to perform tests over the full range of expected and possible temperatures.

5.1.1 Thermal Model Conservatisms

Industry typically employs very conservative assumptions to ensure that they remain within the 400°C regulatory guidance limit established in NRC SFST-ISG-11 Rev. 3 (NRC 2003). A typical example of conservatism in thermal calculations is found in the Calvert Cliffs response to a request for additional information (RAI) from the NRC (Calvert Cliffs 2013). For the design basis loading of a 32P canister at 21.12 total kW, the steady-state PCT during vacuum drying is calculated to be 394°C. This is the same temperature reported during the transfer of the canister to the horizontal storage module if the ambient temperature is 103°F. It should be noted that it takes a very long time for these peak temperatures to be reached; at 110 hours the PCT is still only 383°C. When actual blow down and drying times are used (17.1 to 43.3 hours), even when still assuming the canister is loaded to the 21.12 kW design basis, the temperatures are calculated to be in the range 212°C to 309°C. Since the actual loadings ranged from 11.53 to 18.60 kW (55 to 88 percent of design basis), the actual temperatures would be significantly lower.

Similarly, these conservatisms are illustrated in the calculation of the PCT in the Research Project Cask. As part of the licensing amendment request for the TN-32B cask to be used, the industry team calculated a PCT of approximately 350°C, even though the total decay heat load is above the original design-basis heat load. Using the same decay heats (see Figure 3-3) as input, the thermal modeling team at Pacific Northwest National Laboratory (PNNL) ran COBRA-SFS and STAR-CCM+ and found PCT of 315°C and 324°C, respectively (Fort et al. 2016), when known conservatisms in the industry models were removed. Figure 5-1 shows the PCT and the minimum cladding temperature for each of the 32 assemblies in the Research Project Cask. This confirms the findings in the CASTOR V/21 cask that the peak temperatures in the outer ring of DCSSs can be significantly cooler than those in the central rings, emphasizing the wide axial and radial variability of cladding temperatures.

	270	284	279	267	
267	297	312	312	295	268
275	311	300	315	312	283
283	311	307	301	313	284
271	291	312	312	296	272
	273	284	281	268	

	156	156	156	156	
156	156	157	157	157	156
156	157	158	157	156	156
156	157	156	157	156	156
156	157	157	157	157	156
	158	156	155	156	

Figure 5-1. PCT and Minimum Cladding Temperatures (°C) Predicted by COBRA-SFS for the Project Research Cask Using Decay Heats Provided by Industry (Fort et al. 2016)

Similar analyses performed by Calvert Cliffs (2013), using the actual decay heat loadings, estimated the PCT following helium backfill to be in the range of only 222°C to 265°C. During transfer, using actual decay heat loadings and transfer times and an assumed ambient temperature of 103°F, the PCT ranges from 239°C to 341°C for normal conditions, showing significant margin to the regulatory guidance limit.

When actual decay heat loadings (as opposed to design basis loadings), actual blowdown and drying or transfer times, and actual ambient temperature conditions are used, PCTs are significantly lower than design basis calculations meant to ensure temperatures remain below the regulatory guidance limit. Lower actual temperatures will result in less long-term helium release from fuel pellets, less creep, less hydride dissolution, lower rod internal pressure, and lower hoop stress. However, the time for annealing of radiation damage will be much longer.

5.1.2 Decay Heat Calculations

Another significant source of conservatism when calculating the PCT and other DCSS temperatures is in the decay heat of the individual assemblies. Utilities and cask vendors employ a conservative methodology to determine an assembly decay heat. One approach is to use NRC Regulatory Guide 3.54 (NRC 1999). This methodology uses a number of penalty and safety factors applied to interpolated data to account for bias and uncertainties developed from the comparison of experimental data with calculated values. The goal is to never underestimate the decay heat. Calculated values typically come from using codes such as ORIGEN, using detailed records of conditions during the irradiation of the assembly.

Oak Ridge National Laboratory (ORNL) developed a new method of calculating decay heat (Gauld and Murphy 2010). In this report, they compare the results using Regulatory Guide 3.54 (NRC 1999) and the proposed methodology against experimentally measured values. For PWR assemblies, the Regulatory Guidance 3.54 calculations ranged from 6.8 to 17.2 percent higher than the measured decay heat, with most in the 12 to 15 percent range. For BWR assemblies, the

calculations ranged from 3.7 to 50.5 percent higher than measured values, with the majority well over 15 percent higher.

EPRI developed their Cask Loader database program and evaluated the decay heat calculations within that software system (EPRI 2015b). In this evaluation, they compared the analysis from Cask Loader against ORIGEN calculations. One of the conclusions was that Cask Loader always overestimates the decay heat values when compared to ORIGEN, and such values are therefore considered conservative.

ORNL used detailed irradiation histories to calculate the decay heat of the 32 assemblies at the projected time of loading of the Research Project Cask. The total decay heat was calculated to be 30.6 kW compared to the 36.8 kW using the industry conservative calculations, a decrease of 17 percent. PNNL repeated the thermal analyses using the new decay heats, keeping everything else in the model the same. The results using COBRA-SFS for both the PCT and minimum cladding temperatures are shown in Figure 5-2. Even in these calculations, a number of conservatisms, including assuming a 24-hour average ambient temperature of 100°F (38°C), remain.

	238	247	244	234	
234	257	269	268	256	235
241	268	255	271	269	246
247	268	268	260	269	247
238	255	269	269	257	238
	239	248	246	235	

	138	138	138	138	
138	138	138	138	138	138
138	138	139	138	138	138
138	138	139	139	138	138
138	139	138	138	138	138
	139	138	138	138	

Figure 5-2. PCT and Minimum Cladding Temperatures (°C) Predicted by COBRA-SFS for the Project Research Cask Using Decay Heats Calculated by ORIGEN (Fort et al. 2016)

UFDC continues to evaluate other DCSSs loaded with high burnup fuel to determine the range of PCT. However, based on removing conservatisms in the decay heat calculations, which is the single largest conservatism, and conservatisms in the thermal models, and accounting for actual loading instead of assuming a design basis loading, the highest estimated PCT for all high burnup fuel loaded in a DCSS to date is about 325°C. Note that the conservative approach used in licensing has this PCT approaching 400°C.

To date, UFDC has performed RCT and other tests with a radial hydride treatment of at least 350°C, but most at 400°C. The tests on the sister rods will focus on the range of actual cladding temperatures instead of the assumed upper limit temperatures.

5.2 Hoop Stress

Probably more important than temperature in determining the extent of creep, DHC, or hydride reorientation is the hoop stress in the cladding. The hoop stress depends on the initial helium rod pressure, fission gas release, helium released from alpha decay, the free volume inside the rod after cladding creep down and fuel pellet swelling, and the volume-averaged gas temperature within the fuel rod. Together, these factors determine the EOL RIP that is then related to the hoop stress by a multiplication factor consisting of the cladding metal inner diameter (D_{mi}) and thickness of the cladding metal (h_m): $D_{mi}/(2\ h_{mi})$. Previous RCTs have focused on hoop stresses in the range of 80 to 120 MPa.

The initial helium fill gas pressures have varied over time with initial pressures for PWR rods at room temperature between 1.5 and 3.5 MPa (ASTM 2010). For the 32 assemblies going into the Research Project Cask, the initial pressures are between 1.65 and 2.0 MPa with one older assembly at 2.52 MPa. Lanning and Beyer (2004) showed that initial fill gas pressures at room temperature for 14×14 assemblies was 2.63 MPa. For nominal-fill 15×15 assemblies it was 2.5 MPa and for high-fill 15×15 assemblies it was 3.3 MPa.

Data on the EOL RIP for PWR rods at 25°C are plotted in Figure 5-3. The public database on EOL RIP is quite limited; however, these data are considered representative for standard rods without boron-coated pellets (EPRI 2007; EPRI 2013). For the 17×17 assemblies in Figure 5-3, the initial fill pressure was in the range of 2 to 3.45 MPa. Given the burnup and initial fill pressure, the sister rods would be expected to behave closer to the data at 2 MPa and have EOL RIPs between 4 and 4.5 MPa.

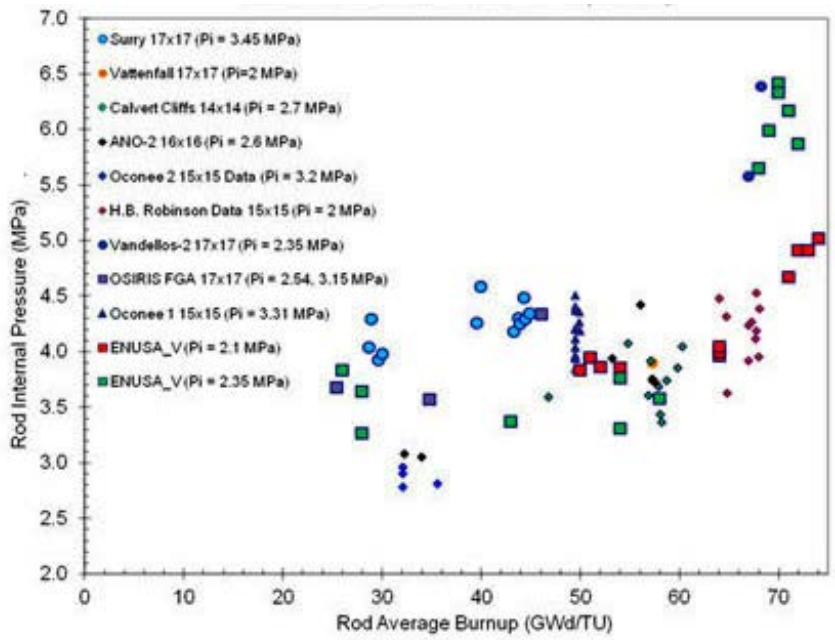

Figure 5-3. End-of-life Rod Internal Pressure for PWR Rods at 25°C (EPRI 2013)

EPRI (2013) used these EOL RIP and void volume data to calculate the number of moles of gas in a rod. They then assumed an axial profile similar to the one measured in the CASTOR V/21 cask with a PCT of 400°C. EPRI calculated a nominal hoop stress of 85 MPa assuming no oxidation of cladding and 92 MPa assuming a 80-µm oxide layer thickness for fuel with a burnup of 60 GWd/MTU.

Lanning and Beyer (2004) performed similar calculations using the FRAPCON-3.2 model assuming a 40-µm oxide layer thickness. They performed calculations assuming PCT of both 570°C and 350°C. These results are presented in Table 5-1. For the lower temperatures, the hoop stresses ranged from 54 to 76 MPa for standard rods, and up to 83 MPa for a 17x17 assembly containing natural boron as an integral fuel burnable absorber (IFBA). Fuel pellets with coatings enriched in B-10 would result in higher helium generation and release, higher RIP values, and higher cladding stresses, but they are still estimated to be less than 93 MPa.

ORNL recently completed a study using FRAPCON-3.5 to look at rod internal pressure quantification, distribution, and hoop stress calculations (Bratton et al. 2015). Bratton et al. specifically modeled over 60,000 rods in the 17×17 assembly designs as irradiated in the Watts Bar Unit 1 reactor. For purposes of illustration and comparison, calculations were performed for a rod-averaged plenum gas temperature of 400°C. The calculated hoop stresses based on EOL RIP are shown in Figure 5-4 for both standard rods and IFBA rods of different designs. The maximum cladding hoop stress for standard rods is 60 MPa at 55 GWd/MTU. This value would decrease if realistic gas temperatures had been used in the calculations.

Table 5-1. End-of-life Hoop Stress for PWR Rods Using FRAPCON (Lanning and Beyer 2004)

Rod Design	BOL Fill Pressure (MPa)	EOL Hoop Stress (MPa)		
		@570°C PCT No oxidation	@570°C PCT 40 µm oxidation	@350°C PCT 40 µm oxidation
B&W 15×15	3.31	89.4	92.8	68.7
Westinghouse 15×15	3.31	98.6	102.8	76.1
Westinghouse 15×15	2.48	79.5	82.9	61.4
CE 14×14	2.63	77.2	80.0	59.3
Westinghouse 14×14	2.63	70.5	73.3	54.3
Westinghouse 17×17 IFBA (natural boron)	NA	NA	112	83
Westinghouse 17×17 IFBA (enriched boron)	NA	NA	<126	<93

BOL = beginning of life, EOL = end of life, IFBA = integral fuel burnable absorber, PCT = peak cladding temperature

UFDC will perform additional analyses to determine the range of hoop stresses to use when performing simulated drying to obtain the t0' conditions. However, it is clear that the lower PCT expected not only in the Research Project Cask but in DCSSs loaded with HBU to date will have a dramatic effect on lowering the hoop stress from the values used in the past.

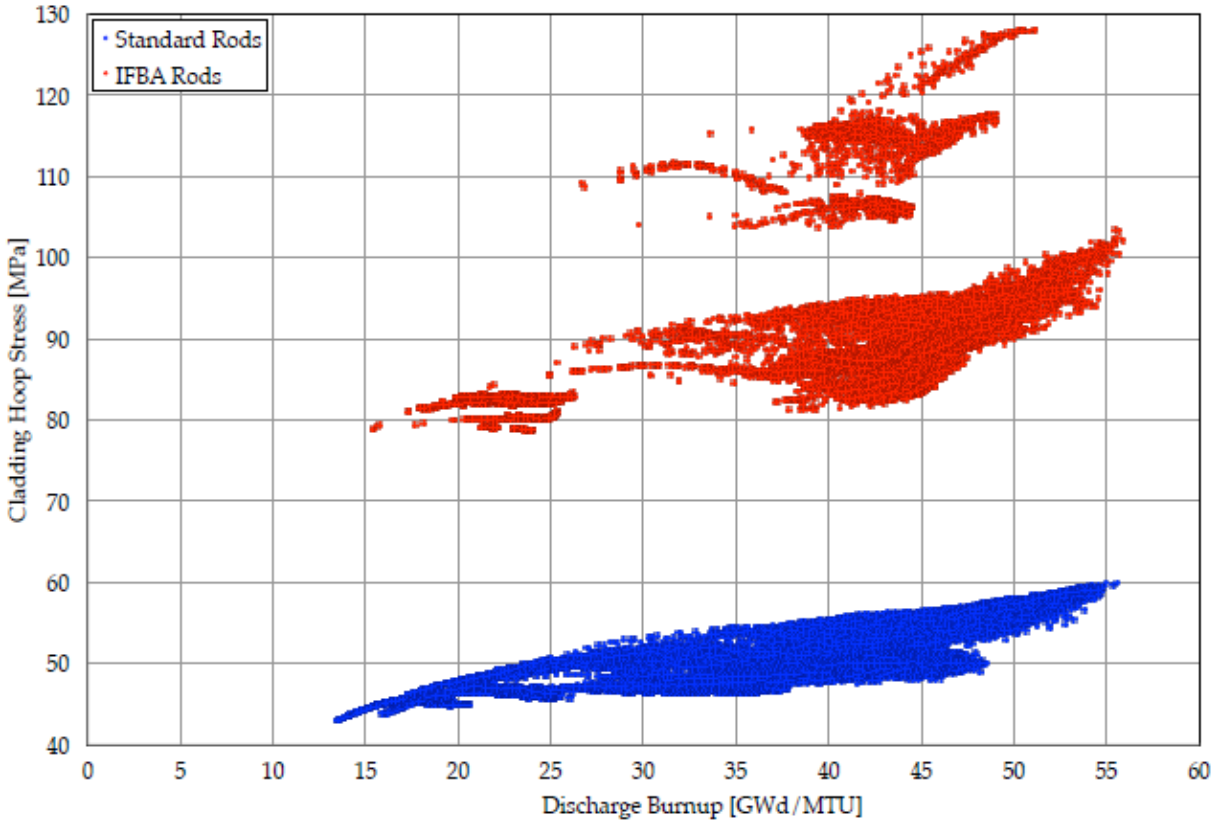

Figure 5-4. Cladding Hoop Stress Predictions for 17×17 Fuel at 400°C PCT (Bratton et al. 2015)

5.3 External Loads

Even if a material is brittle, a sufficient load must be applied in order to cause failure. McConnell et al. (2015) measured the loads expected on cladding under various conditions associated with normal transport. Results to date from shaker table and over-the-road testing are shown in Figure 5-5. The strains observed during the testing are an order of magnitude below those necessary to cause failure when compared to the existing material properties database.

UFDC will continue testing to determine loads expected during extended storage and transportation. In addition, the sister rod testing will determine material properties for the different cladding alloys under t0' conditions to see how they compare with the current database. CIRFT and Transient Shock Testing will be performed using the experimentally determined load to determine fuel performance under a variety of scenarios.

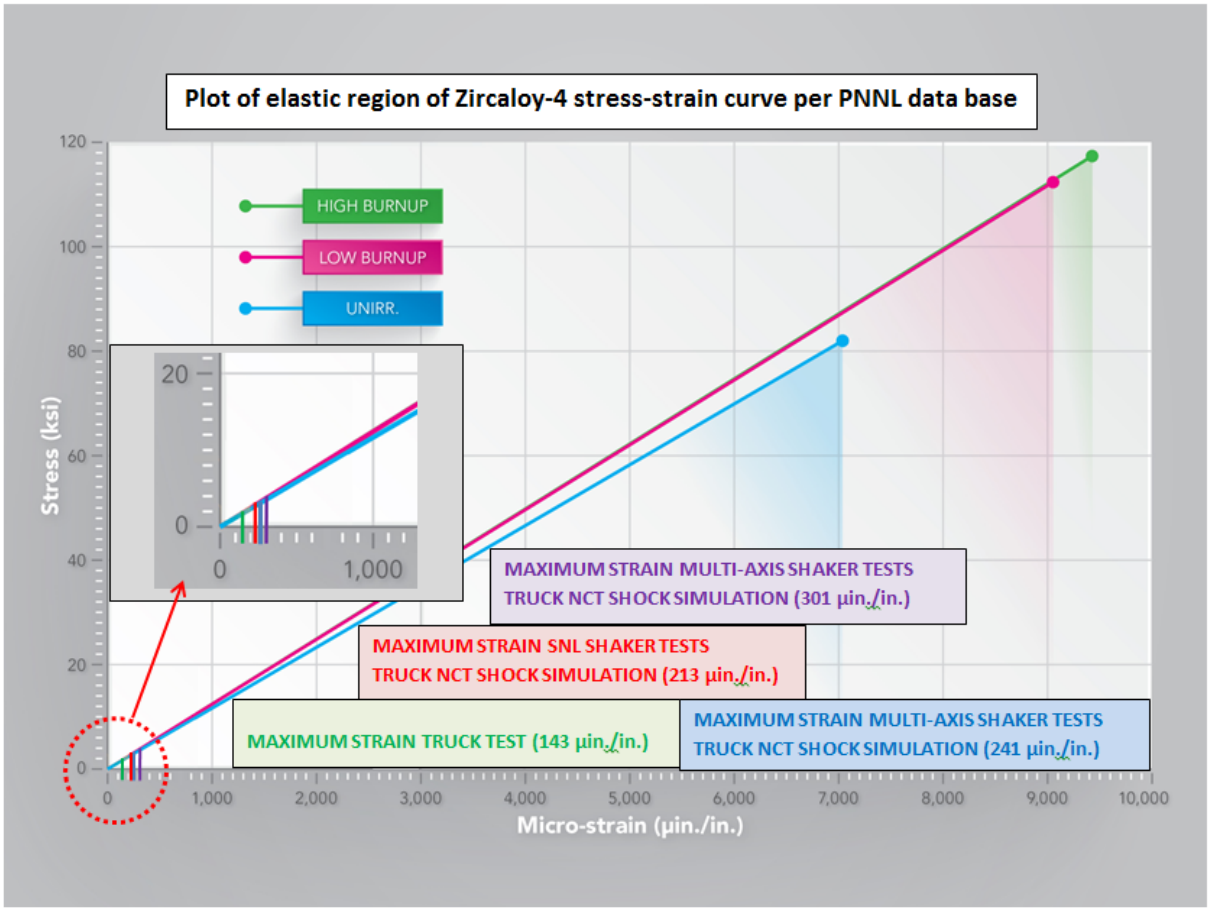

Figure 5-5. Stress-strain Curves for Normal Conditions of Transport (McConnell et al. 2015)

6. SISTER ROD SELECTION

The main purpose of the High Burnup Spent Fuel Data Project is to evaluate the effect of long-term storage on the mechanical properties of HBU SNF. This requires knowing the properties of the fuel as it would be placed in a storage cask/canister and comparing those properties to fuel that has been dried and then stored in a cask/canister for a long period of time. Fuel characterization involves nondestructive (e.g., visual examination, eddy current evaluation, gamma scanning, and metrology) and destructive examination of the fuel (e.g., gas analysis, microscopy, analytical chemistry, and mechanical testing). Destructive examinations impose the requirement to have similar fuel rods for pre- and post-dry storage test examinations. These "sister rods" must have similar characteristics (i.e., same fuel design and cladding, similar in-core operating histories, same cooling times, etc.) as rods to be placed in the TN-32B Research Project Cask. It should be noted that sister rods need not come from the same assembly, a fuel rod with similar characteristics (e.g., irradiation history, symmetric core location, enrichment, and cladding type, etc.) from a different assembly may be determined to be an appropriate "sister" for another fuel rod. Some sister rods will, by necessity, come from fuel assemblies that will not be used in the High Burnup Spent Fuel Data Project.

The two potential fuel assembly sources for sister rods are:

- Assemblies that are going to be placed in the Research Project Cask, or
- Assemblies having similar operating histories (e.g., same batch and symmetric operating histories) to those assemblies that are selected for placement in the Research Project Cask.

For this project, there are only two assemblies that are to be placed in the Research Project Cask that also serve as a donor source for sister rods (assemblies 30A and 5K7). All other sister rods are extracted from assemblies that are not included in the Research Project Cask.

Figure 6-1 shows the loading pattern of assemblies in the Research Project Cask. The map displays the assembly identification number, based on the North Anna convention for tracking fuel assemblies in the spent fuel pool. Within each cell of the grid, the fuel cladding type is also identified, along with the assembly average burnup, initial fuel enrichment, and number of cycles in-core. The age of each assembly (in years since discharge) and the calculated decay heat values as of 7/31/2017 and 1/1/2027 are also shown on the grid. The sister rods selected are shown in Table 6-1.

	1 6T0 Zirlo, 54.2 GWd 4.25%, 3cy, 11yr 1013/819W	2 (TC Lance) 3K7 M5, 53.4 GWd 4.55%, 3cy, 8yr 1167/838W	3 3T6 Zirlo, 54.3 GWd 4.25%, 3cy, 11yr 1015/821W	4 6F2 Zirlo, 51.9 GWd 4.25%, 3cy, 13yr 909/757W	DRAIN PORT
5 3F6 Zirlo, 52.1 GWd 4.25%, 3cy, 13yr 914/762W	6 (TC Lance) 30A M5, 52.0 GWd 4.55%, 3cy, 6yr 1276/832W	7 22B M5, 51.2 GWd 4.55%, 3cy, 5 yr 1637/841W	8 20B M5, 50.5 GWd 4.55%, 3cy, 5 yr 1608/827W	9 5K6 M5, 53.3 GWd 4.55%, 3cy, 8yr 1163/834W	10 5D5 Zirlo, 55.5 GWd 4.2%, 3cy, 17yr 906/797W
11 Vent Port 5D9 Zirlo, 54.6 GWd 4.2%, 3cy, 17yr 885/779W	12 28B M5, 51.0 GWd 4.55%, 3cy, 5 yr 1629/837W	13 F40 Zirc-4, 50.6 GWd 3.59%, 3cy, 30yr 696/ - W	14 (TC Lance) 57A M5, 52.2 GWd 4.55%, 3cy, 6yr 1281/835W	15 30B M5, 50.6 GWd 4.55%, 3cy, 5 yr 1614/830W	16 3K4 M5, 51.8 GWd 4.55%, 3cy, 8 yr 1162/803W
17 5K7 M5, 53.3 GWd 4.55%, 3cy, 8yr 1165/835W	18 50B M5, 50.9 GWd 4.55%, 3cy, 5 yr 1625/835W	19 (TC Lance) 3U9 Zirlo, 53.1 GWd 4.45%, 3cy, 10yr 1037/806W	20 0A4 Low-Sn Zy-4, 50 GWd 4.0%, 2cy, 22yr 725/665W	21 15B M5, 51.0 GWd 4.55%, 3cy, 5 yr 1629/837W	22 6K4 M5, 51.9 GWd 4.55%, 3cy, 8 yr 1162/803W
23 3T2 Zirlo, 55.1 GWd 4.25%, 3cy, 11yr 1036/838W	24 (TC Lance) 3U4 Zirlo, 52.9 GWd 4.45%, 3cy, 10yr 1031/802W	25 56B M5, 51.0 GWd 4.55%, 3cy, 5 yr 1628/837W	26 54B M5, 51.3 GWd 4.55%, 3cy, 5 yr 1645/846W	27 6V0 M5, 53.5 GWd 4.4%, 3cy, 8yrs 1178/844W	28 (TC Lance) 3U6 Zirlo, 53.0 GWd 4.45%, 3cy, 10yr 1035/804W
	29 4V4 M5, 51.2 GWd 4.40%, 3cy, 8yr 1109/787W	30 5K1 M5, 53.0 GWd 4.55%, 3cy, 8yr 1155/829W	31 (TC Lance) 5T9 Zirlo, 54.9 GWd 4.25%, 3cy, 11yr 1031/833W	32 4F1 Zirlo, 52.3 GWd 4.25%, 3cy, 13yr 918/765W	High Priority Assys

Figure 6-1. Final Loading Map Proposed for Research Project Cask (with assembly decay heat estimates provided by Dominion for 7/1/17 and 1/1/27)

Table 6-1. Twenty-five Sister Rods Selected from Seven Assemblies

Clad Material	Donor Assembly Number (3 cycle unless noted)	Donor Rod ID	Key Characteristics	Initial Enrichment (% U-235)	Sister Assembly	Sister Pin
M5	30A	G9	Sister rod to assembly rod in assembly 57A lance position - close proximity to peak (hotest) rod position (I-7) in the cask	4.55	57A	I7
M5	30A	K9	Sister rod to assembly rod in assembly 57A lance position - close proximity to peak (hotest) rod position (I-7) in the cask	4.55	57A	I7
M5	30A	D5	D5 & E14 rods represents locations next to guide tubes that saw burnable poisons (E14) and ones that saw none (D5), this will influence power output during irradiation so pins are expected to have different characteristics even though they have burnups that are very close	4.55	57A	E14
M5	30A	E14	See Rod D5 above	4.55	57A	D5
M5	30A	P2	Next to area with core baffle jetting; based on final location in core for last irradiation cycle	4.55		B2
M5	5K7	P2	Next to area with core baffle jetting; based on final location in core for last irradiation cycle being close to the canister edge in 3K7	4.55	5K6,3K7,5K1	P2
M5	5K7	C5	Equivalent to the rod with peak burnup in othe sister assembly (3K7)	4.55	5K6,3K7,5K1	O13(5K6)
M5	5K7	K9	Sister rod to rod with proximity to thermocouple in assembly (3K7)	4.55	5K6,3K7,5K1	K9(3K7)
M5	5K7	O14	Approximately average assembly burnup	4.55	5K6,3K7,5K1	C-4(5K6)
Zirlo	6U3	I7	this rod mimics the 3 rods that will be isolated and heated to mimic conditions in the cask	4.45	3U4,3U9,3U6	I7(3U4);I11(3U9);I11(3U6)
Zirlo	6U3	M9	Rod is next to a lance position	4.45	3U4,3U9,3U6	E9(3U4)
Zirlo	6U3	K9	Rod is next to a lance position	4.45	3U4,3U9,3U6	K9(3U9)
Zirlo	6U3	L8	Rod is next to a lance position	4.45	3U4,3U9,3U6	F10(3U6)
Zirlo	6U3	O5	Baseline rod at close to max burnup	4.45	3U4,3U9,3U6	C5(3U4);O13(3U9);C13(3U6)
Zirlo	6U3	M3	Basline rod for comparison to 3U4 near max burnup in middle ring zone	4.45	3U4,3U9,3U6	E3(3U4)
Zirlo	6U3	P16	Baseline rod for comparison to rod that should see fastest cooling rate in 3U6 (outer zone)	4.45	3U4,3U9,3U6	B2(3U6)
Zirlo	3F9	N5	Pin for baseline parameters (selected based on matchup with sister assemblies)	4.25	4F1,3F6,6F2	N5(4F1);N5(3F6);N5(6F2)
Zirlo	3F9	D7	Approximately average assembly burnup for baseline parameters	4.25	4F1,3F6,6F2	D7(4F1);D7(3F6);D7(6F2)
Zirlo	3F9	P2	Approximate lowest burnup in assembly and close to edge of assembly	4.25	4F1,3F6,6F2	
Zirlo	3D8	E14	Highest burnup rod in assembly	4.2	5D9,5D5	M4(5D5); N13(5D9)
Zirlo	3D8	B2	Close to lowest burnup rod in assembly (selected based on pulling restriction)	4.2	5D9,5D5	P16(5D5); B16(5D9)
Low tin Zr-4	3A1 (2 cycle)	B16	Lowest burnup rod in assembly; reasonably close to outer edge of assembly	4	OA4*	B16
Low tin Zr-4	3A1 (2 cycle)	F5	Highest burnup rod in assembly; reasonably close to center of assembly	4	OA4*	F5
Zr-4	F35 (4 cycle)	P17	Edge rod (likely to be of most interest from science standpoint)	3.59	None (F40)	
Zr-4	F35 (4 cycle)	K13	Inner region rod for comparison against other Zirc-4 rods (intersting science but limited applicability to discharge population)	3.59	None (F40)	

6.1 Assemblies

The EPRI team proposed the first list of sister assemblies and sister rods. The UFDC reviewed this list and made small modifications to that list based upon additional analyses.

6.1.1 Zircaloy-4 Assemblies

In-pool visual inspection of potential Zircaloy-4 (Zry-4) assemblies (Zry-4 and low-tin Zry-4) found that some of the assemblies being considered could not be included in the cask because of visual characteristics that might indicate excessive corrosion (but not formally confirmed). These assemblies were eliminated from consideration because they were burned for 4 cycles to achieve higher burnup and are not typical of Zry-4 high burnup assemblies.

The Zry-4 assemblies do not have removable top or bottom nozzles, so sister rods cannot be extracted from the assemblies being placed into the demonstration cask. In the case of assembly F40 (Zry-4), there are no true sister rods available, however, as part of a pool-side examination many years ago, several rods from a similar assembly (F35) were removed. While not truly sisters to any rods in F40, the rods from F35 are the best available.

The low-tin Zry-4 assemblies are also in limited supply. Rods are available from assembly 3A1, which is not going in the cask. The assembly has similar characteristics to assembly 0A4 that is going in the cask, but is not truly a sister because it lacks true in-core symmetry. However, 3A1 is the best assembly available as no rods can be pulled from the 0A4 assembly.

6.1.2 M5® Assemblies

Two assemblies were selected as sisters to the AREVA M5® assemblies going in the cask, and, in fact, both these donor assemblies are also going in the cask (assemblies 30A and 5K7). A total of nine sister rods were selected from these two assemblies and this will reduce the heat load of these assemblies slightly (a fact the thermal models will need to account for in the cask thermal analysis).

- Donor assembly 30A will provide sister rods for itself and assembly 57A.
- Donor assembly 5K7 will provide sister rods for itself and assemblies 3K7, 5K1, and 5K6.

6.1.3 ZIRLO® Assemblies

Three assemblies were selected as sisters to the Westinghouse ZIRLO®-clad assemblies going in the cask. A total of 12 sister rods were selected.

- Donor assembly 6U3 will provide sister rods for assemblies 3U4, 3U6, and 3U9.
- Donor assembly 3F9 will provide sister rods for assemblies 3F6, 4F1, and 6F2.
- Donor assembly 3D8 will provide sister rods for assemblies 5D5 and 5D9.

6.1.4 Sister Assembly Locations

Figure 6-2 shows the locations for the thermocouple lances and the locations of each assembly for which there is a sister assembly. Half the assemblies have a sister or similar assembly, while half do not. All assemblies containing thermocouple lances have sisters with the exception of

assembly 5T9. There is a good mix of "outer," "middle," and "inner" assemblies that have sisters: 9 of 16 outer ring assemblies have sisters, 3 of 12 middle assemblies have sisters, and all inner assemblies have sisters or similar assemblies. The designations outer, middle, and inner are related to the assembly loading pattern. This pattern was developed to drive the inner ring to as close as possible to 400°C, the upper regulatory guidance limit for cladding temperatures to ensure cladding integrity is maintained.

6.2 Sister Rods

The sister rods were selected from seven assemblies listed in the second column of Table 6-1. Each assembly and the sister rods selected are discussed in the following sections. Some information about the fuel assemblies and sister rods is considered proprietary by both the nuclear power plant operator, Dominion, and/or the two fuel vendors, AREVA, Inc. and Westinghouse Electric Company, LLC. As a result, some information such as individual fuel rod calculated burnup or location of particular components cannot be discussed. These properties have been reviewed by UFDC personnel under the auspices of specific nondisclosure agreements between the fuel vendors, Dominion, INL, ORNL, and PNNL and those data were considered in the selection of the sister rods.

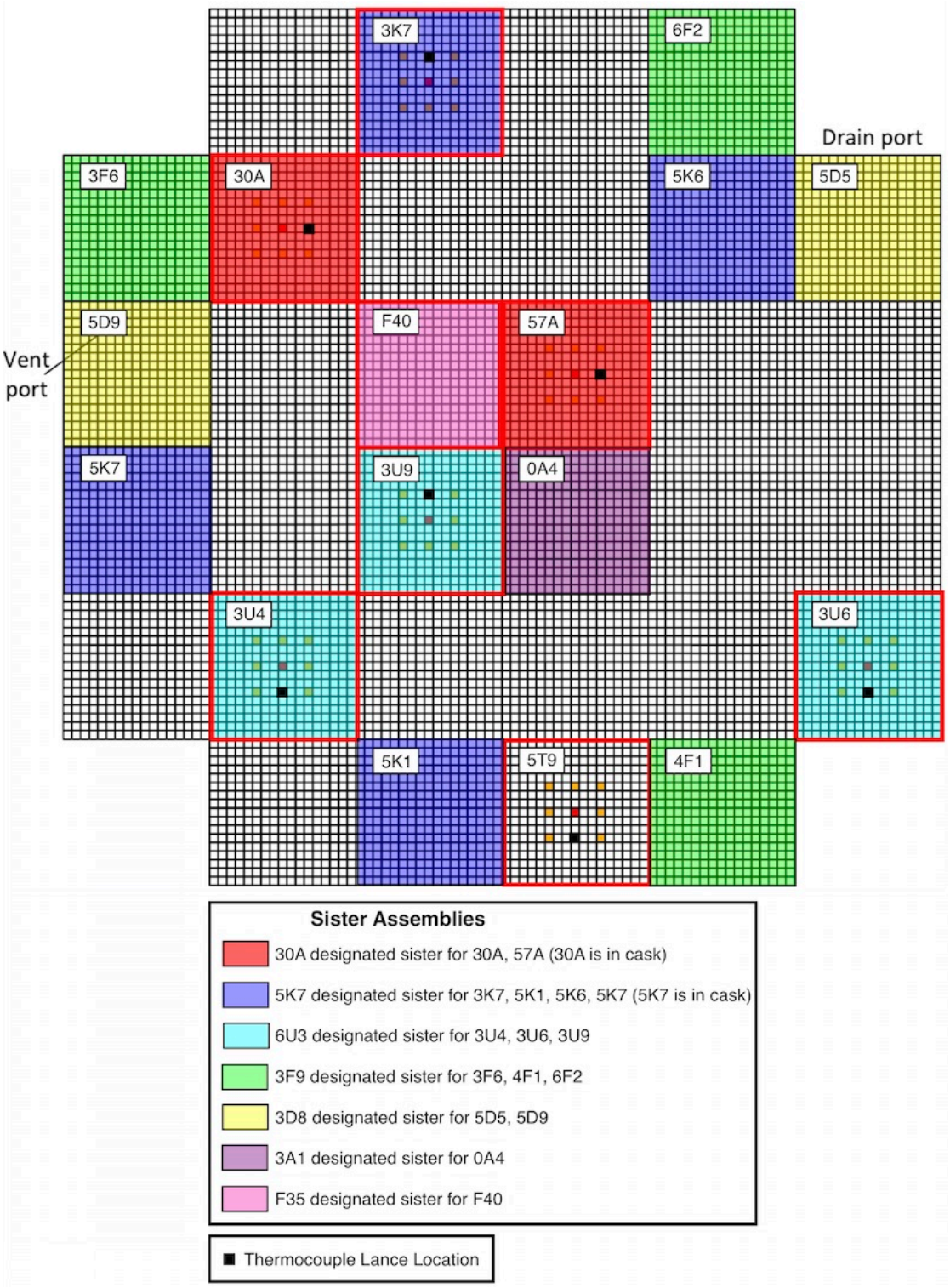

Figure 6-2. Locations of Assemblies in the Research Project Cask that also Have Sister Assemblies are Highlighted. Note assemblies 30A and 5K7 are in the cask and also provide sister rods. All other sister rods come from sister assemblies that are not loaded in the cask.

6.2.1 AREVA M5® Assembly 30A

Assembly 30A is an Advanced Mark BW (AMBW) fuel assembly irradiated at the North Anna Power Station. The cladding is M5® and the initial enrichment of the fuel was 4.55 wt% ^{235}U. This assembly is one that will be placed in the Research Project Cask. It will also provide some rods that are sisters of those in the 30A assembly and also the 57A assembly that will be in the cask. These assemblies and their locations can be seen in Figure 6-2. Figure 6-3 shows in red the locations of the five sister rods that were removed from assembly 30A.

The rods will be described by their map location. For example, the red square in the upper right-hand corner of the fuel assembly is location P2. The letters run vertically, with A on the bottom and Q on the top. The numbers run horizontally from right to left. The black squares represent the location of the guide tubes for control rod insertion with one exception. The black square directly in the middle of the assembly is for the instrument tube. The sister rods selected from this fuel assembly include D5, E14, G9, K9, and P2.

Rod D5 is from a location next to a guide tube that did not have any burnable absorber placed in it over the three cycles of operation. Rod E14 is also from a location next to a guide tube, but in this case burnable absorber was placed in the guide tube at some point during operation. D5 and E14 have similar calculated rod burn-ups, but may have different properties because of the influence of the burnable absorber on E14.

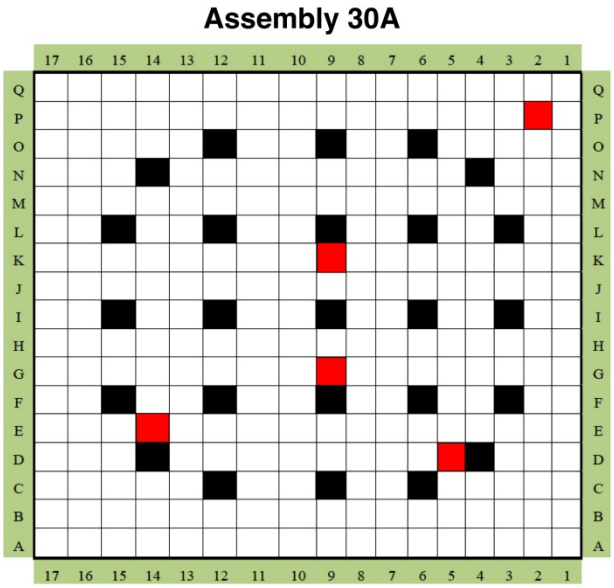

Figure 6-3. Assembly 30A Will Yield Five M5® Sister Rods

Rods G9 and K9 are "related." These two rods are from symmetrical locations within the assembly; both are on the same side of a guide tube, have the same number of fuel rods surrounding them, and have similar burnups. Additionally, both rods would be sisters to rod I7 in assembly 57A that is next to a thermocouple lance. The Research Project Cask provides the first opportunity to measure the temperature at a particular location in a cask as a function of

time and over multiple operations (e.g., water stored in cask, vacuum drying, helium backfill, and establishment of thermal equilibrium). Data from these rods can be confirmed at the end of the Research Project Cask dry storage period when rod I7 can be pulled from assembly 57A.

Rod P2 is near a location in the assembly that may have experienced core baffle jetting as a result of its final location in core during the last irradiation cycle.

6.2.2 AREVA M5® Assembly 5K7

Assembly 5K7 is also an AMBW fuel assembly irradiated at the North Anna Power Station. The cladding is M5® and the initial enrichment of the fuel was 4.55 wt% ^{235}U. This assembly is one that will be placed in the Research Project Cask. It will also serve to provide some rods that are sisters of those in the 5K7 assembly and also the 3K7, 5K1, and 5K6 assemblies that will be in the cask. These assemblies and their locations can be seen in Figure 6-2. Figure 6-4 shows in red the locations of the four sister rods that will be removed from assembly 5K7: C5, K9, O14, and P2.

Rod C5 is equivalent to the rod with the highest (peak) burnup from assembly 3K7. Rod K9 is very similar to the same location in assembly 3K7 and is where a thermocouple lance is located. Rod O14 represents the average assembly burnup for these four sister assemblies (5K7, 3K7, 5K1, and 5K6). Rod P2 is another rod that is located next to an area that may have experienced core baffle jetting during the last cycle of irradiation.

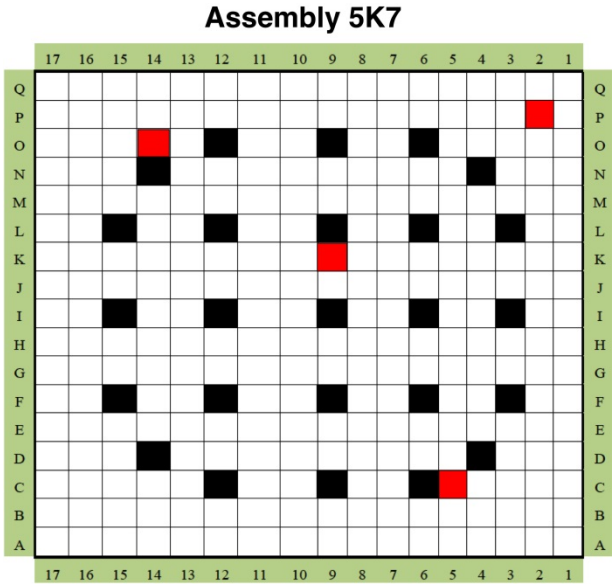

Figure 6-4. Assembly 5K7 Will Yield Four M5® Sister Rods

6.2.3 Westinghouse ZIRLO® Assembly 6U3

Assembly 6U3 is a Westinghouse North Anna Improved Fuel (NAIF) fuel assembly irradiated at the North Anna Power Station. The cladding is ZIRLO® and the initial enrichment of the fuel

was 4.45 wt% ^{235}U. This assembly will not be included in the Research Project Cask, but will serve to provide rods that are sisters of those in 3U4, 3U6, and the 3U9 fuel assemblies that will be placed in the storage cask. These assemblies and their locations can be seen in Figure 6-2; each of these assemblies will have a thermocouple lance. Figure 6-5 shows in red the locations of the seven sister rods that will be removed from assembly 6U3: I7, K9, L8, M3, M9, O5, and P16.

Rods I7, K9, L8, and M9 are all "related," like the rods G9 and K9 are in assembly 30A. Rod I7 is symmetric to the other three rods. The other rods are selected from a position that represents the conditions of fuel near a thermocouple lance location. The difference in the t0 and t0' conditions can be evaluated to determine the effects of the drying process on the fuel condition, and the data from these rods can be confirmed by the corresponding rods that can be pulled from the 3U4, 3U6, and 3U9 assemblies at the end of the cask storage period.

Rod M3 is a rod that can be used to represent a rod of near maximum burnup from assembly 3U4 that is in the "middle" ring of the cask. Rod O5 is representative of other higher burnup rods within the three assemblies. Rod P16 is a rod that can be used to represent a rod that should see the fastest cooling rate in the cask, as will be observed for assembly 3U6 that is in the "outer" ring of the Research Project Cask.

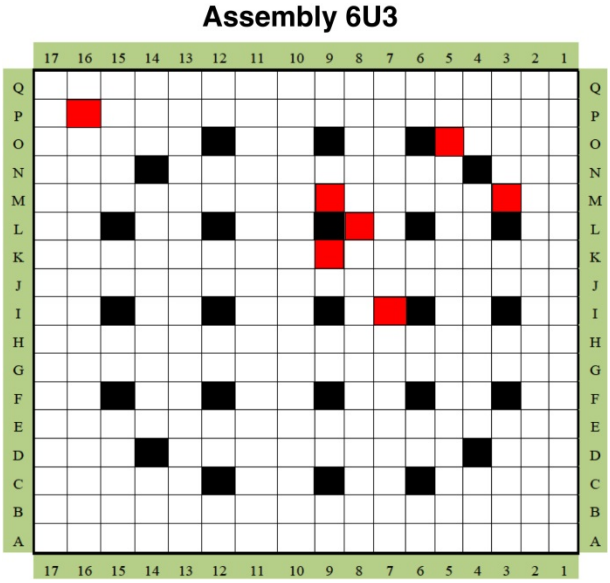

Figure 6-5. Assembly 6U3 Will Yield Seven ZIRLO®-clad Sister Rods Representative of Three Fuel Assemblies that Will be Placed in the Research Project Cask.

6.2.4 Westinghouse ZIRLO® Assembly 3F9

Assembly 3F9 is a Westinghouse NAIF fuel clad with ZIRLO® and the initial enrichment of the fuel was 4.25 wt% ^{235}U. This assembly will not be included in the Research Project Cask. It will provide rods that are sisters of those in 3F6, 4F1, and the 6F2 fuel assemblies that will be placed in the storage cask. These assemblies and their locations can be seen in Figure 6-2; each

of these assemblies are located in corners of the outer ring of fuel and will be expected to cool quickly following vacuum drying. Figure 6-6 shows in red the locations of the three sister rods that will be removed from assembly 3F9: D7, N5, and P2.

Rod D7 is a rod that represents the approximate average burnup for 3F9. Rod N5 is a rod that will be used to represent the baseline properties of the three sister assemblies. Rod P2 is a rod that represents a low burnup rod within the 3F9 assembly.

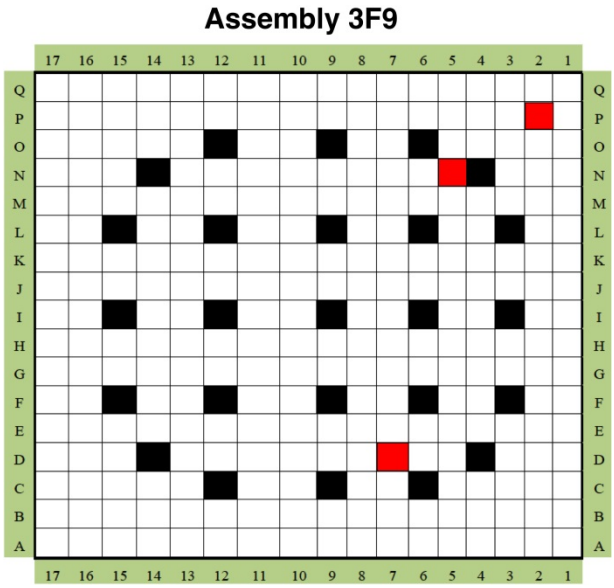

Figure 6-6. Assembly 3F9 Will Yield Three ZIRLO®-clad Sister Rods

6.2.5 Westinghouse ZIRLO® Assembly 3D8

Assembly 3D8 is a Westinghouse NAIF fuel clad with ZIRLO® and the initial enrichment of the fuel was 4.2 wt% ^{235}U. This assembly will not be included in the Research Project Cask. It will provide rods that are sisters of those in 5D5 and the 5D9 fuel assemblies that will be placed in the storage cask. These assemblies and their locations can be seen in Figure 6-2; 5D5 is the assembly near the drain port of the cask and 5D9 is the assembly by the vent port. Both assemblies are in the outer ring of the cask. Figure 6-7 shows in red the locations of the two sister rods that will be removed from assembly 3D8: B2 and E14.

Rod B2 is a rod that represents the lower burnup rods that are found in this and the two sister assemblies. Rod E14 is a rod that represents the higher burnup rods that are found in this and the two sister assemblies.

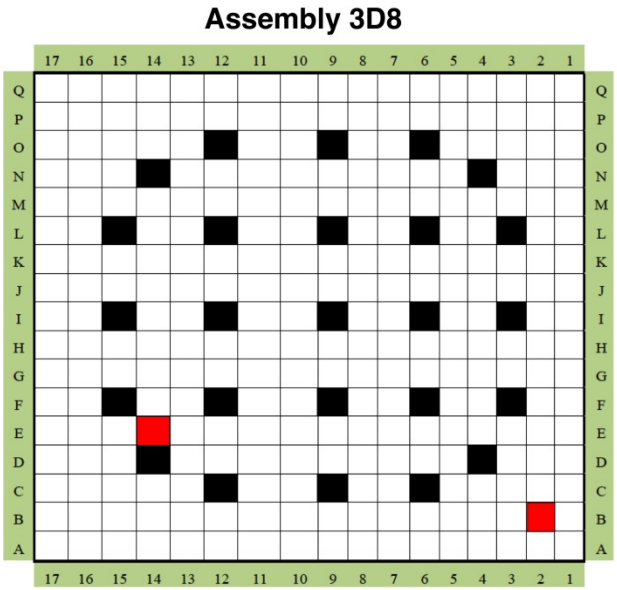

Figure 6-7. Assembly 3D8 Will Yield Two ZIRLO®-clad Sister Rods

6.2.6 Westinghouse Low-Tin Zircaloy-4 Assembly 3A1

Assembly 3A1 is a Westinghouse NAIF fuel clad with low-tin Zircaloy-4 and the initial enrichment of the fuel was 4 wt% ^{235}U. This assembly was irradiated in two reactor cycles. This assembly will not be included in the Research Project Cask. It will serve to provide rods that are similar to those in assembly 0A4. These rods are not true sisters to those in 0A4 because of differences in irradiation history, but there is a limited inventory of high burnup low-tin Zircaloy-4 assembles. The location of the 0A4 assembly is shown in Figure 6-2; 0A4 is in the inner ring of the cask that should be in the highest temperature region of the cask. Figure 6-8 shows in the locations of the two sister rods that will be removed from assembly 3A1: B16 and F5.

Rod B16 is a rod that represents the lower burnup rods that are found in this assembly. Rod F5 is a rod that represents the higher burnup rods that are found in this assembly.

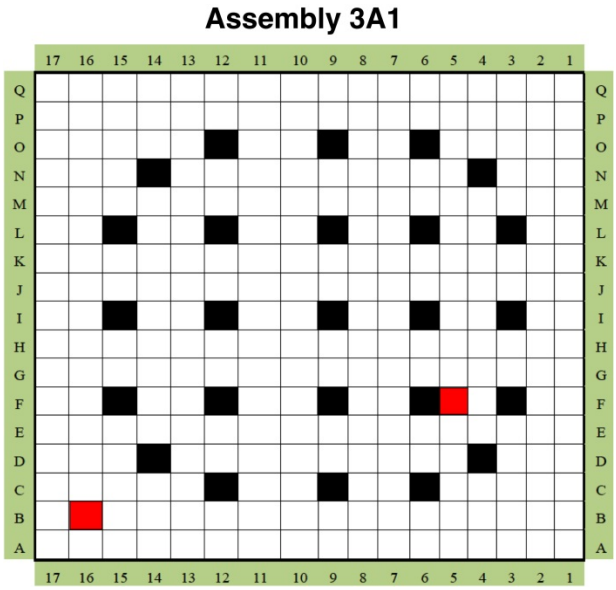

Figure 6-8. Assembly 3A1 Will Yield Two Low-tin Zircaloy-4-clad Rods

6.2.7 Westinghouse Zircaloy-4 Assembly F35

Assembly F35 is a Westinghouse LOPAR[1] assembly with the fuel clad with Zircaloy-4. The initial enrichment of the fuel was 3.59 wt% ^{235}U. The assembly was irradiated in four reactor cycles to achieve high burnup. This assembly will not be included in the Project Research Cask. It will serve to provide rods that are similar to those in assembly F40. These rods are not true sisters to those in F40 due to differences in irradiation history, but because of the fuel assembly design, there is no way to pull rods in what has come to be a conventional manner (removing the top nozzle and pulling rods out the top of the assembly). The rods from F35 were pulled during a pool-side examination campaign performed many years ago at the North Anna spent fuel pool. These rods were pulled out the bottom of the fuel assembly and have been stored in the pool ever since.

The location of the F40 assembly is shown in Figure 6-2; F40 is in the inner ring of the cask that should be in the highest temperature region of the cask. Figure 6-9 shows in red the locations of the two sister rods that were removed from assembly F35: K13 and P17.

Rod K13 is from the inner area of the F35 fuel assembly. Rod P17 is from the outer edge of the assembly. These rods are expected to yield some bounding high burnup characteristic information about Zircaloy-4 cladding, information on an assembly edge rod, and perhaps some baseline information about this obsolete assembly's performance in storage (i.e., the Zircaloy-4 cladding is being replaced by different alloys as fuel goes to higher burnups).

[1] The Westinghouse LOPAR fuel assembly design was patented in 1974 and was named "low parasitic" (LOPAR) because it was designed having a relatively small amount of parasitic structural material in the grids and support structure for the guide tubes.

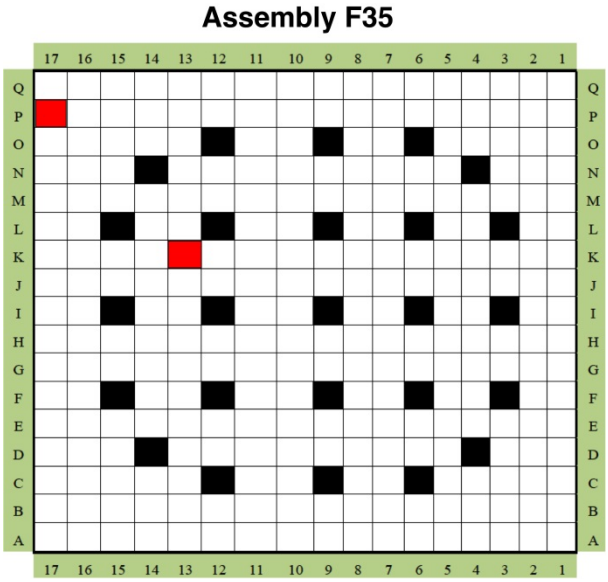

Figure 6-9. Assembly F35 Will Yield Two Zircaloy-4-clad Rods

7. REFERENCES

10 CFR Part 72. Licensing Requirements for the Independent Storage of Spent Nuclear Fuel and High-Level Radioactive Waste. U.S. Nuclear Regulatory Commission, Washington, D.C.

42 U.S. C. 10101 et seq. *The Nuclear Waste Policy Act of 1982*. Public Law 97-425 as amended.

Adamson R, F Garzarolli, A Strasser, P Rudling, and G Wikmark. 2004. *High Burnup Fuel Issues. IZNA-3 Special Topics Report.* Advanced Nuclear Technology International, Göteborg, Sweden.

ASTM. 2010. *Standard Guide for the Evaluation of Materials Used in Extended Service of Interim Spent Nuclear Fuel Dry Storage Systems*. ASTM C1562-10. ASTM International, West Conshohocken, Pennsylvania.

Billone MC, TA Burtseva, and MA Martin-Rengel. 2015. *Effects of Lower Drying-Storage Temperatures on the DBTT of High-Burnup PWR Cladding.* FCRD-UFD-2015-000008. ANL-15/21. Prepared for the U.S. Department of Energy Used Fuel Disposition Campaign, Washington, D.C.

Billone MC, TA Burtseva, and RE Einziger. 2013. "Ductile-to-brittle transition temperature for high-burnup cladding alloys exposed to simulated drying-storage conditions." *Journal of Nuclear Materials,* 433:431-448.

Bouffioux P, A Ambard, A Miquet, C Cappelaere, Q Auzoux, M Bono, O Rabouille, S Allegre, V Chabretou, and CP Scott. 2014. "Hydride Reorientation in M5® Cladding and Its Impact on Mechanical Properties." In proceedings, *LWR Fuel Performance Meeting (TopFuel 2013), September 15-19, 2013, Charlotte, North Carolina*, p. 879. Curran Associates, Inc., Red Hook, New York.

Bratton RN, MA Jessee, and WA Wieselquist. 2015. *Rod Internal Pressure Quantification and Distribution Analysis Using FRAPCON*. FCRD-UFD-2015-000636. ORNL/TM-2015/557. Oak Ridge National Laboratory. Oak Ridge, Tennessee.

Brémier S, CT Walker, and R Manzel. 2001. "Fission Gas Release and Fuel Swelling at Burn-ups Higher than 50 MWd/kgU." In *Fission Gas Behavior in Water Reactor Fuels, Seminar Proceedings, Cadarache, France, 26-29 September 2000*. Nuclear Energy Agency, Organization for Economic Co-Operation and Development, Paris.

Calvert Cliffs. 2013. Calvert Cliffs Response For RAI#E-3, Calvert Cliffs Nuclear Power Plant, LLC, April 24, 2013. Available at https://adamswebsearch2.nrc.gov/webSearch2/view?AccessionNumber=ML13119A243.

Croff AG. 1980. *ORIGEN-2—A Revised and Updated Version of the Oak Ridge Isotope Generation and Depletion Code.* ORNL-5621. Oak Ridge National Laboratory, Oak Ridge, Tennessee.

EIA. 2016. "Nuclear and Uranium, Spent Nuclear Fuel, Table 3 Annual commercial spent fuel discharges and burnup 1968- June 2013." U.S. Energy Information Administration. Accessed at https://www.eia.gov/nuclear/spent_fuel/ussnftab3.cfm on April 4, 2016.

Einziger RE and C Beyer. 2007. "Characteristics and Behavior of High-Burnup Fuel That May Affect the Source Terms for Cask Accidents." *Nuclear Technology,* 159(2):134-146.

EPRI. 2015a. "Session #4: Technical Issues Cladding." Presented by Albert Machiels at 2015 Division of Spent Fuel Management (DSF) Regulatory Conference (REG CON 2015), Washington, D.C. November 18-19, 2015. Available at http://www.nrc.gov/public-involve/conference-symposia/dsfm/2015/dsfm-2015-albert-machiels.pdf.

EPRI. 2015b. *Evaluation of Cask Loader Decay Heat Calculations.* 3002005503. Electric Power Research Institute, Palo Alto, California.

EPRI. 2014. *High Burnup Dry Storage Cask Research and Development Project: Final Test Plan*. Contract No.: DE-NE-0000593. Electric Power Research Institute, Palo Alto, California.

EPRI. 2013. *End-of-Life Rod Internal Pressures in Spent Pressurized Water Reactor Fuel*. Report Number 3002001949. Electric Power Research Institute, Palo Alto, California.

EPRI. 2012. *Impacts Associated with Transfer of Spent Nuclear Fuel from Spent Fuel Storage Pools to Dry Storage After Five Years of Cooling, Revision 1*. TR-1025206. Electric Power Research Institute, Palo Alto, California.

EPRI. 2010. *Impacts Associated with Transfer of Spent Nuclear Fuel from Spent Fuel Storage Pools to Dry Storage After Five Years of Cooling.* TR-1021049, Electric Power Research Institute, Palo Alto, California.

EPRI. 2007. *Spent Fuel Transportation Applications – Assessment of Cladding Performance: A Synthesis Report.* 1015048. Electric Power Research Institute, Palo Alto, California.

EPRI. 2002. *Dry Cask Storage Characterization Project*. TR-1002882. Electric Power Research Institute, Palo Alto, California.

EPRI. 2001. *Optimum Cycle Length and Discharge Burnup for Nuclear Fuel: Phase I: Results Achievable Within the 5% Enrichment Limit.* TR-1003133. Electric Power Research Institute, Palo Alto, California.

EPRI. 1986. *The CASTOR-V/21 PWR Spent –Fuel Storage Cask: Testing and Analysis*, EPRI NP-4887, Electric Power Research Institute. Palo Alto, California.

Exelon Generation. 2015. *Calvert Cliffs Nuclear Power Plant Independent Spent Fuel Storage Installation Site-Specific License Second Request for Additional Information, Part 2*. Docket No. 72-8. September 11, 2015. Available at https://adamswebsearch2.nrc.gov/webSearch2/view?AccessionNumber=ML15258A194.

Exelon Generation. 2010. *Calvert Cliffs Nuclear Power Plant Independent Spent Fuel Storage Installation Site-Specific License Renewal Application.* Docket No. 72-8. September 17, 2010. Found at http://pbadupws.nrc.gov/docs/ML1026/ML102650247.pdf.

Fort JA, JM Cuta, SR Suffield, and HE Adkins. 2016. *Thermal Modeling of Proposed TN-32B Cask for High Burnup Fuel Storage Demonstration Project.* FCRD-UFD-2015-000116, PNNL-24549 Rev. 1. Prepared for the U.S. Department of Energy Used Fuel Disposition Campaign, Washington, D.C.

Gauld IC and BD Murphy. 2010. *Technical Basis for a Proposed Expansion of Regulatory Guide 3.54-Decay Heat Generation in an Independent Spent Fuel Storage Installation.* NUREG/CR-6999. ORNL/TM-2007/231. Prepared for the U.S. Nuclear Regulatory Commission Office of Nuclear Regulatory Research, Washington, D.C.

Geelhood K and C Beyer. 2013. *Used Nuclear Fuel Loading and Structural Performance under Normal Conditions of Transport – Supporting Material Properties and Modeling Inputs.* FCRD-UFD-2013-000123. Prepared for the U.S. Department of Energy Used Fuel Disposition Campaign, Washington, D.C.

Hanson B, H Alsaed, C Stockman, D Enos, R Meyer, and K Sorenson. 2012a. *Gap Analysis to Support Extended Storage of Used Nuclear Fuel*. FCRD-USED-2011-000136 Rev. 0, PNNL-20509. Prepared for the U.S. Department of Energy Used Fuel Disposition Campaign, Washington, D.C.

Hanson B, H Alsaed, and C Stockman. 2012b. *Used Nuclear Fuel Storage and Transportation Data Gap Prioritization*. FCRD-USED-2012-000109 DRAFT, PNNL-21360. Prepared for the U.S. Department of Energy Used Fuel Disposition Campaign, Washington, D.C.

Hanson BD, RC Daniel, AM Casella, RS Wittman, W Wu, PJ MacFarlan, and RW Shimskey. 2008. *Fuel-In-Air FY07 Summary Report*. PNNL-17275 Rev. 1. Pacific Northwest National Laboratory, Richland, Washington.

Ito K, K Kamimura, and Y Tsukuda. 2004. "Evaluation of Irradiation Effect on Spent Fuel Cladding Creep Properties." In *Proceedings of the 2004 International Meeting on LWR Fuel Performance*, p. 440. American Nuclear Society, La Grange Park, Illinois.

Johnson L, C Ferry, C Poinssot, and P Lovera. 2005. "Spent fuel radionuclide source-term model for assessing spent fuel performance in geological disposal. Part I: Assessment of the instant release fraction." *Journal of Nuclear Materials*, 346:56-65.

Kim YS. 2008. "Delayed Hydride Cracking of Spent Fuel Rods in Dry Storage." *Journal of Nuclear Materials* 378:30-34.

Klymyshyn NA, NP Barrett, KI Johnson, and BD Hanson. 2015. *Update: Structural Uncertainty of Used Nuclear Fuel in Dry Storage Canisters.* FCRD-UFD-2015-000493, PNNL-24669. Prepared for the U.S. Department of Energy Used Fuel Disposition Campaign, Washington, D.C.

Koo Y-H, B-H Lee, J-S Cheon, and D-S Sohn. 2001. "Pore pressure and swelling in the rim region of LWR high burnup UO_2 fuel." *Journal of Nuclear Materials*, 295:213-220.

Lanning DD and CE Beyer. 2004. *Estimated Maximum Cladding Stresses for Bounding PWR Fuel Rods During Short Term Operations for Dry Cask Storage.* Available at http://pbadupws.nrc.gov/docs/ML0402/ML040290474.pdf.

Manzel R and CT Walker. 2000. "High burnup fuel microstructure and its effect of fuel rod performance." In proceedings of the ANS Topical Meeting on *Light Water Reactor Fuel Performance*, Park City, Utah.

Mardon JP, GL Garner, and PB Hoffman. 2010. "M5® a breakthrough in Zr alloy." In Proceedings of *2010 LWR Fuel Performance/TopFuel/WRFPM*. Orlando, Florida. September 26-29, 2010. American Nuclear Society.

McConnell P, G Koenig, W Uncapher, C Grey, C Engelhardt, S Saltzstein, and K Sorenson. 2015. *Surrogate Fuel Assembly Multi-Axis Shaker Tests to Simulate Normal Conditions of Rail and Truck Transport.* FCRD-UFD-2015-000128. Prepared for the U.S. Department of Energy Used Fuel Disposition Campaign, Washington, D.C.

NRC. 2015. NRC license renewal to Northern States Power Company-Minnesota for Prairie Island Nuclear Generating Plant Independent Spent Fuel Storage Installation. December 16, 2015. Available at http://www.regulations.gov/#!documentDetail;D=NRC-2013-0251-0008.

NRC. 2014. NRC license renewal to Exelon Generation Corporation, LLC for Calvert Cliffs Independent Spent Fuel Storage Installation. October 23, 2014. Available at https://www.federalregister.gov/articles/2014/10/29/2014-25758/exelon-generation-corporation-llc-calvert-cliffs-independent-spent-fuel-storage-installation.

NRC. 2012. *Burnup Credit in the Criticality Safety Analyses of PWR Spent Fuel in Transport and Storage Casks*. SFST-ISG-8, Rev 3. U.S. Nuclear Regulatory Commission, Washington, D.C.

NRC. 2010. *Standard Review Plan for Spent Fuel Dry Storage Systems at a General License Facility*. NUREG-1536, Rev 1. U.S. Nuclear Regulatory Commission, Washington, D.C.

NRC. 2005. *Encl2 – Safety Evaluation Report to 02/25/05 Ltr D Christian, Virginia Electric and Power Co, Issuance of Renewed Materials License No. SNM-2501, Surry Independent Spent Fuel Storage Installation (72-1) (L23091).* U.S. Nuclear Regulatory Commission, Washington, D.C.

NRC. 2003. *Cladding Considerations for the Transportation and Storage of Spent Fuel*. SFST-ISG-11, Rev 3. U.S. Nuclear Regulatory Commission, Washington, D.C.

NRC. 1999. *Regulatory Guide 3.54. Spent Fuel Heat Generation in an Independent Spent Fuel Storage Installation. Rev. 1.* U.S. Nuclear Regulatory Commission, Washington, D.C.

Pan G, AM Garde, AR Atwood, R Källström, and D Jädernäs. 2013. "High Burnup Optimized ZIRLO™ Cladding Performance." In *LWR Fuel Performance Meeting TopFuel 2013, September 15-19, 2013, Charlotte, North Carolina*. American Nuclear Society.

Raynaud PAC, and RE Einziger. 2015. "Cladding stress during extended storage of high burnup spent nuclear fuel." *Journal of Nuclear Materials.* 464:304-312.

Stockman CT, BD Hanson, SC Marschman, HA Alsaed, and KB Sorenson. *Used Nuclear Fuel Extended Storage and Transportation Research and Development Review and Plan, Revision 1*. FCRD-USED-2014-000050 Rev. 1, SAND2014-19594 R. Prepared for the U.S. Department of Energy Used Fuel Disposition Campaign, Washington, D.C.

Strasser A, K Sheppard, L Goldstein, and S Rajan. 1986. *"Extended Burnup Potential and Plant Capacity Factor Savings of Improved LWR Fuel Designs"*, Symposium on Water Reactor Fuel Technology and Utilization, Stockholm, September, 1986. International Atomic Energy Agency, Vienna.

Wang JA, H Wang, H Jiang, Y Yann, and BB Bevard. 2015. *FY 2015 Status Report: CIRFT Testing of High-Burnup Used Nuclear Fuel Rods from Pressurized Water Reactor and Boiling Water Reactor Environments.* M2-FCRD-UFD-2015-000101 (ORNL/SPR-2015/313). Oak Ridge National Laboratory, Oak Ridge, Tennessee.

Xcel Energy. 2011. *Prairie Island Independent Spent Fuel Storage Installation Site-Specific License Renewal License Application.* Docket No. 72-10. October 20, 2011. Available at http://pbadupws.nrc.gov/docs/ML1130/ML11304A068.pdf.